INTERNATIONAL JOURNAL FOR NUMERICAL METHODS IN FLUIDS
Int. J. Numer. Meth. Fluids 2007; **53**:573–597
Published online 24 July 2006 in Wiley InterScience (www.interscience.wiley.com). DOI: 10.1002/fld.1295

On stabilized finite element methods for the Stokes problem in the small time step limit

Pavel B. Bochev[1,*,†], Max D. Gunzburger[2,‡] and Richard B. Lehoucq[1,§]

[1]*Computational Mathematics and Algorithms Department, Sandia National Laboratories, Mail Stop 1110, Albuquerque, New Mexico 87185-1110, U.S.A.*
[2]*School of Computational Science, Florida State University, Tallahassee FL 32306-4120, U.S.A.*

SUMMARY

Recent studies indicate that consistently stabilized methods for unsteady incompressible flows, obtained by a method of lines approach may experience difficulty when the time step is small relative to the spatial grid size. Using as a model problem the unsteady Stokes equations, we show that the semi-discrete pressure operator associated with such methods is not uniformly coercive. We prove that for sufficiently large (relative to the square of the spatial grid size) time steps, implicit time discretizations contribute terms that stabilize this operator. However, we also prove that if the time step is sufficiently small, then the fully discrete problem necessarily leads to unstable pressure approximations. The semi-discrete pressure operator studied in the paper also arises in pressure-projection methods, thereby making our results potentially useful in other settings. Copyright © 2006 John Wiley & Sons, Ltd.

Received 22 December 2005; Revised 11 May 2006; Accepted 14 May 2006

KEY WORDS: stabilized finite element methods; unsteady Stokes equations; small time step limit; SVD; inf–sup

*Correspondence to: Pavel B. Bochev, Computational Mathematics and Algorithms Department, Sandia National Laboratories, Mail Stop 1110, Albuquerque, New Mexico 87185-1110, U.S.A.
†E-mail: pbboche@sandia.gov
‡E-mail: gunzburg@csit.fsu.edu
§E-mail: rblehou@sandia.gov

Contract/grant sponsor: U.S. Department of Energy's National Nuclear Security Administration; contract/grant number: DE-AC-94AL85000
Contract/grant sponsor: Computer Science Research Institute, Sandia National Laboratories; contract/grant number: 18407

1. INTRODUCTION

Stable and accurate mixed finite element methods for incompressible flows require pressure and velocity approximations that satisfy the inf–sup (or LBB) compatibility condition [1, 2]. Among other things, this condition prevents the use of standard, equal-order C^0 elements defined with respect to the same grid or low order pairs such as piecewise linear velocities and piecewise constant pressures. Finite difference analogues of such pairs are collocated velocity–pressure and nodal velocity-cell centred pressure schemes that are also unstable. Stabilized mixed methods [3–11] circumvent the inf–sup condition and enable incompressible flow calculations using a wider choice of velocity–pressure pairs. This offers advantages such as uniform data structures, local conservation, and algebraic equations that are easier to solve by iterative methods. For this reason, stabilized methods are in widespread use for the discretization of the steady-state and time-dependent Navier–Stokes equations and related problems.

Stabilized methods for steady-state problems add terms that make the variational equation coercive, or weakly coercive, for spaces that fail to satisfy the inf–sup condition; see References [3, 12, 13] for general discussions. In this paper, we focus on *consistently stabilized* methods that achieve stabilization by using residuals of the differential equations. When properly weighted, these residuals provide the needed stabilization terms and at the same time vanish for the exact solution so that the formal order of accuracy of the Galerkin method is preserved.

Stabilized methods for time-dependent problems are commonly defined by using a method of lines approach whereby the spatial and temporal discretization steps are separated; see References [14–17]. Stabilization terms are introduced in the semi-discrete (in space) equation by using residuals of the *time-dependent* partial differential equation. In this approach, stabilization strategies for unsteady problems are directly inherited from successful stabilization strategies used for steady-state problems. The stabilized (in space) semi-discrete equation is then discretized in time by a suitable time-stepping scheme. In particular, as far as stability is concerned, the time step of an implicit time integrator method can be chosen large relative to the spatial grid size. However, there are at least two settings in which the desired time step is much smaller than the spatial grid size and for which the aforesaid methods do not perform as well as one would expect (relative to their performance for larger time steps and for steady-state problems). First, in problems involving chemical reactions, the size of the time step is often governed by the reaction rates. Thus, accuracy considerations would suggest the use of a relatively large spatial grid size but a relatively smaller time step is needed in order to account for the stiffness due to the reactions. Second, temporal and spatial discretization algorithms of disparate orders of accuracy require that the errors due to the two discretization steps be balanced by choosing correspondingly disparate time steps and spatial grid sizes.

Complications in consistently stabilized methods arising from small time steps were reported in References [18, 19]. The analysis found in Reference [19] established that spatial stabilization in conjunction with finite differencing in time introduces destabilizing terms and that $\Delta t > \alpha h^2$ (where α is a sufficiently large positive constant, Δt denotes the times step and h some measure of the spatial grid size) is a sufficient condition to avoid instabilities. Although the analysis in Reference [19] remained inconclusive on the necessity of this condition, computational examples in References [18, 19] strongly suggest that this is indeed the case.

We remark that although the use of relatively small time steps can result from the need to accurately resolve transients due to fast reactions and/or strong advection, the small time step problems encountered with stabilized methods for incompressible flows are not directly due to

DOI: 10.1002/fld

the appearance of reaction terms[¶] or nonlinear terms in the differential equations. As a result, it suffices to use as a model problem the unsteady Stokes equations.

Our paper demonstrates how the use of a time-dependent residual for the *velocity–pressure pair* stabilization leads to a semi-discrete pressure operator that is unstable, or equivalently, is not uniformly (with respect to h) coercive. This is a new result that explains why fully discrete formulations experience problems in the $\Delta t \to 0$ limit. In contrast to the analyses of References [18, 19] where the main focus was on the coercivity of the fully discrete stabilized variational equation, here we start with the properties of the stabilized semi-discrete equation for the unsteady Stokes flow. Then, we show that implicit discretization in time results in the pressure operator acquiring additional terms that stabilize the fully discrete equations *provided* $\Delta t/\tau > \alpha$ where τ is the stabilization parameter and $\alpha > 0$ is independent of h and Δt. This necessary stability condition implies that in the small time step limit τ must scale as $O(\Delta t)$. On the other hand, to provide velocity–pressure stabilization τ must scale as $O(h^2)$. These are contradicting requirements that cannot be satisfied unless Δt and h are such that $\Delta t/h^2 > \alpha$. This is a significant improvement over the result of Reference [19] because a lower bound on the ratio of temporal and spatial discretization steps is *necessary* for stability, but can be otherwise chosen arbitrarily. The matrix operator studied in this paper arises in other approaches such as exact or approximate pressure-projection methods [25]. This makes our findings potentially useful to a wider range of methods and discretization techniques for incompressible flows.

We have organized this paper as follows. A brief summary of notations ends this section. In Section 2, we review stabilized mixed methods for the stationary Stokes problem. Section 3 extends these methods to the unsteady Stokes equations. Then, in Section 4, motivating computational examples illustrating small time-step pressure instabilities are provided. The main result of this paper is found in Section 5 where we prove that the semi-discrete pressure operator is not uniformly coercive. The fully discrete pressure-Poisson stabilized systems are defined and studied in Section 6 where we show that the discretized in time pressure operator is conditionally stable and derive a necessary stability condition in the form of a lower bound on the time step. Section 7 extends the main results in Sections 5 and 6 to two other stabilized formulations. In Section 8 we briefly comment on a connection with pressure-projection methods. Our conclusions are summarized in Section 9.

1.1. Notations

We let $H^k(\Omega)$, $\|\cdot\|_k$, $|\cdot|_k$ and $(\cdot,\cdot)_k$ denote the Sobolev space of all square integrable functions with square integrable derivatives up to order k, and the standard Sobolev norm, seminorm and

[¶] Stabilized methods for scalar advection–diffusion–reaction and diffusion–reaction equations have been developed in References [20–23]. In contrast to the stabilized methods considered in this paper, where the goal is to avoid the inf–sup compatibility condition between the velocity and pressure approximations, such methods aim to stabilize the weak Galerkin form associated with the singularly perturbed operator $-\varepsilon\triangle\phi + \sigma\phi$. Solutions of such equations may have boundary layers where standard Galerkin methods will develop spurious oscillations. Recently, Harari [24] used the reaction–diffusion model to explain some pathologies arising in the numerical solution of the heat equation by an implicit time integration. He pointed out that for sufficiently small time steps and implicit discretization in time, the fully discrete heat equation is similar to a finite element approximation of a singularly perturbed elliptic problem. Accordingly, stabilized methods designed for reaction–diffusion problems can be applied to stabilize the fully discrete heat equation at the small time step limit. In contrast, in this paper we consider a pathology that is caused by the velocity–pressure stabilization itself and that cannot be remedied unless the time step is large enough, because the associated semi-discrete equation is not well-posed.

DOI: 10.1002/fld

inner product, respectively. The domain Ω denotes a simply connected bounded region in $\mathbf{R}^d$, $d=2,3$, with a sufficiently smooth boundary Γ. The space $L^2(\Omega)$ denotes $H^0(\Omega)$ and so we drop the zero from the inner product designation. As usual, $H_0^1(\Omega)=\{v\in H^1(\Omega)\mid v=0 \text{ on } \Gamma\}$ and $L_0^2(\Omega)=\{q\in L^2(\Omega)\mid \int_\Omega q\,\mathrm{d}\Omega=0\}$. Spaces of vector-valued functions are denoted by boldface notation so that $\mathbf{H}^1(\Omega)$ is the space of vector-valued functions whose components belong to $H^1(\Omega)$. Matrices and vectors are denoted by upper-case letters such as $\mathbb{A}$ and A, respectively. The time interval of interest is designated as $(0,T)$ with $T>0$. In this paper, we consider continuous piecewise polynomial finite element spaces defined with respect to a regular [26] partition $\mathscr{T}_h$ of the domain Ω into finite elements $\mathscr{K}$. For example, $\mathscr{K}$ can be a hexahedron or tetrahedron in three dimensions or a triangle or quadrilateral in two dimensions.

2. STABILIZED MIXED GALERKIN METHODS FOR THE STEADY-STATE STOKES EQUATIONS

In the method of lines approach for unsteady problems, a spatial discretization is followed by a finite difference approximation in time. In this paper, we focus on finite element methods for which the spatial discretization is obtained by extending a class of *consistently* stabilized mixed methods for the steady-state Stokes problem

$$\begin{aligned} -\triangle\mathbf{u}+\nabla p&=\mathbf{f} \quad \text{in } \Omega\\ \nabla\cdot\mathbf{u}&=0 \quad \text{in } \Omega\\ \mathbf{u}&=\mathbf{0} \quad \text{on } \Gamma \end{aligned} \tag{1}$$

to the time-dependent equations. This section provides a concise summary of the relevant stabilized methods for (1).

Let $\mathscr{V}_h\subset\mathbf{H}_0^1(\Omega)$ and $\mathscr{P}_h\subset L_0^2(\Omega)$ denote a conforming velocity–pressure finite element pair for (1). An (unstabilized) mixed finite element method [2] for (1) is given by: seek $(\mathbf{u}_h,p_h)\in\mathscr{V}_h\times\mathscr{P}_h$ such that

$$G(\{\mathbf{u}_h,p_h\},\{\mathbf{v}_h,q_h\})=(\mathbf{f},\mathbf{v}_h)\quad \text{for all } (\mathbf{v}_h,q_h)\in\mathscr{V}_h\times\mathscr{P}_h \tag{2}$$

where

$$G(\{\mathbf{u}_h,p_h\},\{\mathbf{v}_h,q_h\})=(\nabla\mathbf{u}_h,\nabla\mathbf{v}_h)-(p_h,\nabla\cdot\mathbf{v}_h)-(q_h,\nabla\cdot\mathbf{u}_h) \tag{3}$$

is the mixed Galerkin variational form. Let $\{\boldsymbol{\xi}_i^h\}_{i=1}^K$ and $\{\chi_i^h\}_{i=1}^M$ denote bases for $\mathscr{V}_h$ and $\mathscr{P}_h$, respectively, so that

$$\mathbf{u}_h(\mathbf{x})=\sum_{j=1}^K U_j\boldsymbol{\xi}_j^h(\mathbf{x})\quad\text{and}\quad p_h(\mathbf{x})=\sum_{j=1}^M P_j\chi_j^h(\mathbf{x}) \tag{4}$$

Then, the weak variational equation (2) is equivalent to the matrix problem

$$\begin{pmatrix}\mathbb{A} & \mathbb{B}^{\mathrm{T}}\\ \mathbb{B} & 0\end{pmatrix}\begin{pmatrix}U\\ P\end{pmatrix}=\begin{pmatrix}F\\ 0\end{pmatrix} \tag{5}$$

DOI: 10.1002/fld

where the jth components of U and P are U_j and P_j, respectively. The matrices $\mathbb{A} \in \mathbf{R}^{K\times K}$ and $\mathbb{B} \in \mathbf{R}^{M\times K}$ are defined in the usual manner from the terms in the Galerkin mixed form (3) and represent the stiffness and divergence matrices. Their entries in the ith row and jth column are given by

$$\mathbb{A}_{ij} = (\nabla \boldsymbol{\xi}_i^h, \nabla \boldsymbol{\xi}_j^h) \quad \text{and} \quad \mathbb{B}_{ij} = -(\chi_i^h, \nabla \cdot \boldsymbol{\xi}_j^h) \tag{6}$$

respectively. In a similar fashion, F is defined from the source term $\mathbf{f}$ in (2), i.e. $F_i = (\mathbf{f}, \boldsymbol{\xi}_i^h)$.

The second equation of (5) implies that the velocity is discretely divergence free (or discretely solenoidal) which, in the context of finite element methods, simply means that

$$(q_h, \nabla \cdot \mathbf{u}_h) = 0 \quad \text{for all } q_h \in \mathscr{P}_h$$

The variational equation (2), or equivalently, the linear system (5) are stable if and only if the finite element pair $(\mathscr{V}_h, \mathscr{P}_h)$ satisfies the inf–sup condition [1, 2, 27]

$$\inf_{q_h\in\mathscr{P}_h, q_h\neq 0} \sup_{\mathbf{v}_h\in\mathscr{V}_h, \mathbf{v}_h\neq \mathbf{0}} \frac{(q_h, \nabla\cdot \mathbf{v}^h)}{\|\mathbf{v}_h\|_1 \|q_h\|_0} = \kappa_h \geqslant \kappa_h^{\min} > 0 \tag{7}$$

where $\kappa_h^{\min}$ is independent of the grid size h. This is equivalent to the condition that the matrix $\mathbb{B}$ is uniformly, with respect to $h \to 0$, of full row rank; see References [3, 28–30].

Many popular and/or simple choices for $(\mathscr{V}_h, \mathscr{P}_h)$ fail to satisfy the inf–sup condition (7). Such is the case if the velocity–pressure pair consists of equal-order, C^0 elements defined with respect to the same partition $\mathscr{T}_h$ of Ω into finite elements and also if $(\mathscr{V}_h, \mathscr{P}_h)$ is the piecewise linear (or bilinear)-piecewise constant pair; see References [1, 2] for details. The primary motivation for the use of stabilized methods is to allow for a stable and accurate approximation of (1) by such pairs. In doing so, the class of admissible pairs for incompressible flow calculations is extended to finite element spaces that offer additional computational advantages such as uniform data structures or local mass conservation.

In this paper we consider only *consistently* stabilized methods for (1); these are formulations that are exactly satisfied by the solutions of the Stokes problem (1). They are also the ones that are in most common use because they retain the formal approximation order of (2). Consistently stabilized methods have the following general form: seek $(\mathbf{u}_h, p_h) \in \mathscr{V}_h \times \mathscr{P}_h$ such that

$$G(\{\mathbf{u}_h, p_h\}, \{\mathbf{v}_h, q_h\}) + \langle R_m(\mathbf{u}_h, p_h), W_m(\mathbf{v}_h, q_h)\rangle_m$$

$$+ \langle R_c(\mathbf{u}_h, p_h), W_c(\mathbf{v}_h, q_h)\rangle_c = (\mathbf{f}, \mathbf{v}_h) \tag{8}$$

for all $(\mathbf{v}_h, q_h) \in \mathscr{V}_h \times \mathscr{P}_h$, where

$$R_m(\mathbf{u}_h, p_h)|_{\mathscr{K}} = -\triangle \mathbf{u}_h + \nabla p_h - \mathbf{f} \quad \text{and} \quad R_c(\mathbf{u}_h, p_h)|_{\mathscr{K}} = \nabla \cdot \mathbf{u}_h$$

are *element* residuals of the Stokes equations (1), $W_m(\mathbf{v}_h, q_h)$ and $W_c(\mathbf{v}_h, q_h)$ are *weighting* functions, and $\langle\cdot,\cdot\rangle_m$ and $\langle\cdot,\cdot\rangle_c$ are *discrete* inner products. To avoid technical complications that are irrelevant to our study, in what follows we restrict attention to equal order C^0 velocity–pressure pairs. A common choice for such pairs is to set

$$W_c(\mathbf{v}_h, q_h) = 0, \quad W_m(\mathbf{v}_h, q_h) = -\gamma \triangle \mathbf{v}_h - \nabla q_h \quad \text{and} \quad \langle \mathbf{u}_h, \mathbf{v}_h\rangle_m = \sum_{\mathscr{K}\in\mathscr{T}_h} \tau_{\mathscr{K}}(\mathbf{u}_h, \mathbf{v}_h)_{\mathscr{K}}$$

DOI: 10.1002/fld

where γ can take on the values ± 1 or 0 and $\tau_{\mathscr{K}}$ are positive, real stabilization parameters. Noting that $\langle \cdot, \cdot \rangle_m$ is a 'broken' L^2 inner product (broken into a sum of inner products over the individual elements), the weak equation (8) takes the form: seek $(\mathbf{u}_h, p_h) \in \mathscr{V}_h \times \mathscr{P}_h$ such that

$$G(\{\mathbf{u}_h, p_h\}, \{\mathbf{v}_h, q_h\}) - \sum_{\mathscr{K} \in \mathscr{T}_h} \tau_{\mathscr{K}} (-\triangle \mathbf{u}_h + \nabla p_h - \mathbf{f}, -\gamma \triangle \mathbf{v}_h + \nabla q_h)_{\mathscr{K}} = (\mathbf{f}, \mathbf{v}_h) \tag{9}$$

for all $(\mathbf{v}_h, q_h) \in \mathscr{V}_h \times \mathscr{P}_h$. For $\gamma = 1, 0, -1$, the method (9) is, respectively, known as the *Galerkin-least-squares* [10], the *pressure-Poisson stabilized Galerkin* [11], and the *Douglas–Wang* [7] method; see Reference [3] for a review. A standard choice of stabilization parameters is

$$\tau_{\mathscr{K}} = \delta h_{\mathscr{K}}^2 \tag{10}$$

where $h_{\mathscr{K}}$ is a measure of the element size and $\delta > 0$ is a real parameter that is independent of $h_{\mathscr{K}}$ but whose values may be restricted in order to guarantee the stability of the discrete problem (9); see References [3, 8]. We refer to (10) as the *spatial* τ; see References [31, 32].

3. STABILIZED SEMI-DISCRETE FORMULATIONS OF THE UNSTEADY STOKES EQUATIONS

The time-dependent Stokes equations are given by

$$\begin{aligned} \frac{\partial \mathbf{u}}{\partial t} - \triangle \mathbf{u} + \nabla p &= \mathbf{f} \quad \text{in } \Omega \times (0, T) \\ \nabla \cdot \mathbf{u} &= 0 \quad \text{in } \Omega \times (0, T) \\ \mathbf{u} &= \mathbf{0} \quad \text{on } \Gamma \times (0, T) \\ \mathbf{u}|_{t=0} &= \mathbf{u}_0 \quad \text{in } \Omega \end{aligned} \tag{11}$$

with velocity $\mathbf{u}(\mathbf{x}, t)$ and pressure $p(\mathbf{x}, t)$, where $\mathbf{f}(\mathbf{x}, t)$ and $\mathbf{u}_0(\mathbf{x})$ are given functions.

In a method of lines approach, to obtain the semi-discrete formulation of (11) we express the approximate solution as

$$\mathbf{u}_h(\mathbf{x}, t) = \sum_{j=1}^{K} U_j(t) \boldsymbol{\xi}_j^h(\mathbf{x}) \quad \text{and} \quad p_h(\mathbf{x}, t) = \sum_{j=1}^{M} P_j(t) \chi_j^h(\mathbf{x}) \tag{12}$$

where, as before, $\{\boldsymbol{\xi}_i^h\}_{i=1}^K$ and $\{\chi_i^h\}_{i=1}^M$ span a conforming velocity–pressure pair $\mathscr{V}_h \subset \mathbf{H}_0^1(\Omega)$ and $\mathscr{P}_h \subset L_0^2(\Omega)$, respectively. The main difference between (4) and (12) is that now the coefficients of the finite element approximations are time-dependent. An (unstabilized) mixed finite element semi-discretization of (11) is defined as follows: seek $\mathbf{u}_h(\cdot, t) \in \mathscr{V}_h$ and $p_h(\cdot, t) \in \mathscr{P}_h$ such that

$$(\dot{\mathbf{u}}_h(\cdot, t), \mathbf{v}_h) + G(\{\mathbf{u}_h(\cdot, t), p_h(\cdot, t)\}, \{\mathbf{v}_h, q_h\}) = (\mathbf{f}(\cdot, t), \mathbf{v}_h) \tag{13}$$

$$(\mathbf{u}_h(\cdot, 0), \mathbf{v}_h) = (\mathbf{u}_0, \mathbf{v}_h) \tag{14}$$

DOI: 10.1002/fld

for all $(\mathbf{v}_h, q_h) \in \mathscr{V}_h \times \mathscr{P}_h$ and $t \in (0, T)$. The semi-discrete equation (13) is equivalent to the differential-algebraic equation (DAE)

$$\begin{pmatrix} \mathbb{M}\dot{U} \\ 0 \end{pmatrix} + \begin{pmatrix} \mathbb{A} & \mathbb{B}^{\mathrm{T}} \\ \mathbb{B} & 0 \end{pmatrix} \begin{pmatrix} U \\ P \end{pmatrix} = \begin{pmatrix} F \\ 0 \end{pmatrix} \tag{15}$$

and the initial condition (14) is equivalent to the linear algebraic system

$$\mathbb{M}U(0) = U_0 \tag{16}$$

In (15) and (16), $U(t) = \{U_1(t), \ldots, U_K(t)\}$ and $P(t) = \{P_1(t), \ldots, P_M(t)\}$ are the vectors of unknown coefficients corresponding to $\mathbf{u}_h(\mathbf{x}, t)$ and $p_h(\mathbf{x}, t)$, respectively. The matrix $\mathbb{M} \in \mathbf{R}^{K \times K}$ is defined in the usual manner from the first term in (13) and represents the consistent mass matrix having the entry in the ith row and jth column given by

$$\mathbb{M}_{ij} = (\boldsymbol{\xi}_i^h, \boldsymbol{\xi}_j^h) \tag{17}$$

Similarly, the vectors $F(t)$ and U_0 are defined from the source term $\mathbf{f}$ and the initial data $\mathbf{u}_0$, respectively, i.e. $F_i = (\mathbf{f}, \boldsymbol{\xi}_i^h)$ and $(U_0)_i = (\mathbf{u}_0, \boldsymbol{\xi}_i^h)$.

If $(\mathscr{V}_h, \mathscr{P}_h)$ satisfies (7), then (13) and (14) or, equivalently, the DAE (15) and (16), is a spatially stable problem for any time $t > 0$. On the other hand, if $(\mathscr{V}_h, \mathscr{P}_h)$ does not satisfy (7), which is the case when one uses equal-order, C^0 elements defined on the same grid, then the mixed Galerkin form $G(\cdot, \cdot)$ in (13) is unstable and this equation will not, in general, produce accurate approximations at any time $t > 0$. To enable the use of unstable velocity–pressure pairs in the spatial discretization of (11), the mixed Galerkin form $G(\cdot, \cdot)$ must be properly stabilized.

Our study focuses on formulations that extend the consistently stabilized family of methods (9) to the time-dependent Stokes equations. We will refer to such algorithms as *spatially stabilized methods*. A simple and obvious way to stabilize the semi-discrete equation (13) is to add the same terms as in (9). However, if $\mathbf{u}$ is an unsteady solution of (13) and (14), then $-\Delta\mathbf{u} + \nabla p - \mathbf{f} = -\dot{\mathbf{u}} \neq 0$ and so the modified semi-discrete equation will no longer be consistent. To fulfill the consistency requirement, stabilization terms can be introduced by using the full time-dependent residual:

$$-\sum_{\mathscr{K} \in \mathscr{T}_h} \tau_{\mathscr{K}} \left(\dot{\mathbf{u}}_h(\cdot, t) - \Delta\mathbf{u}_h(\cdot, t) + \nabla p_h(\cdot, t) - \mathbf{f}(\cdot, t), -\gamma\Delta\mathbf{v}_h + \nabla q_h\right)_{\mathscr{K}}$$

This results in the following *modified* semi-discrete equation: seek $\mathbf{u}_h(\cdot, t) \in \mathscr{V}_h$ and $p_h(\cdot, t) \in \mathscr{P}_h$ such that (14) and

$$\begin{aligned} &(\dot{\mathbf{u}}_h(\cdot, t), \mathbf{v}_h) + G(\{\mathbf{u}_h(\cdot, t), p_h(\cdot, t)\}, \{\mathbf{v}_h, q_h\}) - (\mathbf{f}(\cdot, t), \mathbf{v}_h) \\ &\quad - \sum_{\mathscr{K} \in \mathscr{T}_h} \tau_{\mathscr{K}} \left(\dot{\mathbf{u}}_h(\cdot, t) - \Delta\mathbf{u}_h(\cdot, t) + \nabla p_h(\cdot, t) - \mathbf{f}(\cdot, t), -\gamma\Delta\mathbf{v}_h + \nabla q_h\right)_{\mathscr{K}} = 0 \end{aligned} \tag{18}$$

hold for all $(\mathbf{v}_h, q_h) \in \mathscr{V}_h \times \mathscr{P}_h$ and $t \in (0, T)$. An alternative definition of τ for time dependent problems and uniform grids is given by [31, 32]

$$\tau = \left(\left(\frac{2}{\Delta t} \right)^2 + \frac{1}{(\delta h^2)^2} \right)^{-1/2} \tag{19}$$

To distinguish this definition from (10) we refer to (19) as the *transient* τ.

DOI: 10.1002/fld

The modified problem (18) is consistent in the sense that any sufficiently smooth solution $(\mathbf{u}(\mathbf{x}, t), p(\mathbf{x}, t))$ of (11) satisfies (18). The consistency requirement is fulfilled by the inclusion of the weighted time derivative term

$$-\sum_{\mathscr{K}\in\mathscr{T}_h} \tau_{\mathscr{K}}(\dot{\mathbf{u}}_h, -\gamma\triangle\mathbf{v}_h + \nabla q_h)_{\mathscr{K}} \tag{20}$$

in (18). Our main concern, however, lies with the well-posedness of this equation. While

$$-\sum_{\mathscr{K}\in\mathscr{T}_h} \tau_{\mathscr{K}}(-\triangle\mathbf{u}_h + \nabla p_h - \mathbf{f}, -\gamma\triangle\mathbf{v}_h + \nabla q_h)_{\mathscr{K}} \tag{21}$$

contributes the same terms that were sufficient to stabilize the *steady* mixed Galerkin equation (2), it is not clear whether or not the combination of (20) and (21) makes the modified semi-discrete equation (18) uniformly stable with respect to h.

Our studies in References [18, 19] suggest that (18) may not be well-behaved. We found that the fully discrete equations become unstable when the time step Δt is sufficiently small compared to the mesh size h. However, analyses based on the fully discrete problem only allowed us to show that $\Delta t > \alpha h^2$, where α is sufficiently large, is a *sufficient* stability condition. In this paper, we take a different approach and base our analysis on the semi-discrete problem. We are motivated by the fact that in the limit $\Delta t \to 0$, a fully discrete formulation approaches (18). Therefore, stability problems observed through the fully discrete equations at the small time step limit may in fact be due to the inherent instability of (18) itself.

4. MOTIVATING COMPUTATIONAL EXPERIMENTS

We now provide a sample of the experiments that motivated us to consider the behaviour of stabilized finite element methods for the unsteady Stokes equations in the small time step limit. We plot the pressure field obtained after a *single step* of the backward-Euler method applied to (18) with $\gamma = 0$ and τ defined by (10), i.e. we consider an extension of the pressure-Poisson stabilization to the time-dependent setting using the spatial τ. The initial data $\mathbf{u}_0$ and source term $\mathbf{f}$ are generated by the time independent exact solution

$$\mathbf{u} = \mathbf{curl}\,\psi \quad \text{and} \quad p = \sin(x)\cos(y) + (\cos(1) - 1)\sin(1) \tag{22}$$

where $\psi(x, y) = x^2(1 - x)^2 \sin^2(\pi y)$. This choice of $\mathbf{u}$ ensures that (1) $\mathbf{u}$ is solenoidal and that (2) $\mathbf{u}$ satisfies the homogeneous boundary condition in (1). The right-hand side of the momentum equation corresponding to (22) is given by

$$\mathbf{f} = \begin{pmatrix} 2\pi(-1 + 6x + 2(\pi^2 - 3)x^2 - 4\pi^2 x^3 + 2\pi^2 x^4)\sin(2\pi y) + \cos(x)\cos(y) \\ 4\pi^2 x(1 - 3x + 2x^2)\cos(2\pi y) - 12(1 - 2x)\sin^2(\pi y) - \sin(x)\sin(y) \end{pmatrix}$$

The hydrostatic pressure mode is eliminated by fixing the pressure value at a single grid node. We note that this reduces convergence by a logarithmic factor in two dimensions and by one order in three dimensions [33]. However, the goal of our study is the small time step behaviour rather than spatial convergence and so this simple method is acceptable. If $(\mathbf{u}_h, p_h)$ is a solution of the steady-state stabilized Stokes problem (9) with $\gamma = 0$, then $(\mathbf{u}_h, p_h)$ is also a solution of the fully

DOI: 10.1002/fld

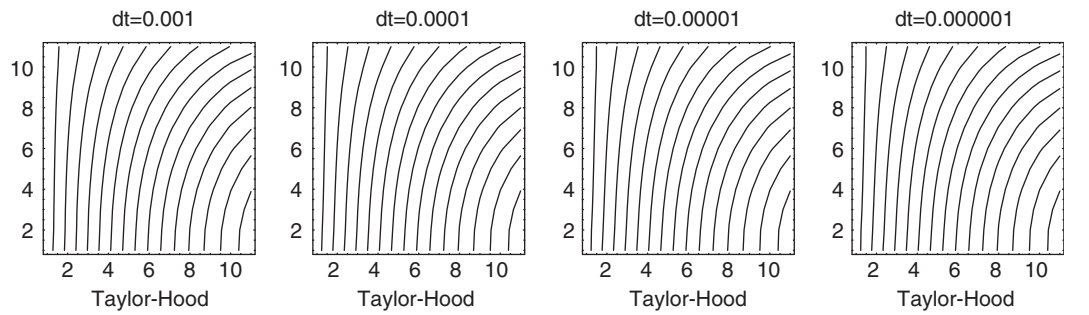

Figure 1. Approximate pressure in the $\Delta t \to 0$ limit for the Taylor–Hood element pair and $n = 3, 4, 5, 6$. The tick marks denote node numbers in x (horizontal axis) and y (vertical axis) directions.

discrete problem obtained from (18) (with the same value of γ). Therefore, if $\mathbf{u}_h^0$ is computed by (16), after one time step, the unsteady approximation $(\mathbf{u}_h^1, p_h^1)$ should be an $O(\Delta t)$ perturbation of the steady-state solution $(\mathbf{u}_h, p_h)$. Thus, for small Δt, these two solutions are indistinguishable, that is, $(\mathbf{u}_h^1, p_h^1)$ should be *unchanged* as we reduce the time step.

In the experiments, Ω is the unit square, $\mathscr{T}_h$ is a uniform triangulation consisting of 200 triangles, and the time steps are $(\Delta t)_n = 10^{-n}$ for $n = 3, 4, 5, 6$. For this mesh, $h = 0.1$ and $h^2 = 0.01$ so that $(\Delta t)_k < h^2$. On two occasions, we also use the time step $(\Delta t)_1 = 10^{-1}$ that is larger than h^2. To provide a reference solution, we solve (13) using the stable Taylor–Hood element pair, the same spatial grid, the same time integration method, and the same time steps. Figure 1 shows that p_h is an accurate approximation of the exact pressure that does not change as the time step is reduced from $(\Delta t)_3$ to $(\Delta t)_6$. We conclude that the Taylor–Hood pair remains stable when $\Delta t < h^2$.

On uniform grids we can use the same value of $\tau_{\mathscr{K}}$ on all elements. As a result, for the stabilized method, we only need to select the parameter δ in (10). In Reference [3], the value $\delta = 0.05$ was found to be optimal in numerical convergence studies on uniform grids. We use this value to compute the stabilized solution for the four time steps and equal order P1–P1, P2–P2, and P3–P3 velocity–pressure pairs. The top row in Figure 2 shows the approximate pressure p_h for P1–P1 elements after one time step. As the time step decreases from $(\Delta t)_3$ to $(\Delta t)_6$, p_h appears to converge to a state that is not an accurate approximation of the true solution (22). We recall that for linear elements, the term $-\triangle \mathbf{u}_h$ in (18) vanishes and the stabilizing contribution of the spatial term (21) defaults to $\sum_{\mathscr{K}} \tau_{\mathscr{K}} (\nabla p_h, \nabla q_h)_{\mathscr{K}}$. This gives an *inconsistently* stabilized method similar to the one described in Reference [34], and so some loss of accuracy is to be expected. Specifically, the Neumann condition on the pressure is induced by the term $\sum_{\mathscr{K}} \tau_{\mathscr{K}} (-\Delta \mathbf{u}_h, \nabla q_h)_{\mathscr{K}}$. For linear elements this term vanishes and so the pressure is subjected to an incorrect homogeneous Neumann condition.

The middle row in Figure 2 shows p_h for P2–P2 elements. One step of the backward-Euler method with $(\Delta t)_3$ leaves p_h essentially unchanged. However, as the time step decreases, the pressure approximations begin to deviate from the exact solution, with the deviation being strongest for the smallest time step. We note that this happens in a fairly smooth manner.

For the P3–P3 pair, the pressure behaviour is markedly different. The bottom row in Figure 2 shows no substantial variations in p_h for $(\Delta t)_3$ and $(\Delta t)_4$. However, reducing the time step to $(\Delta t)_5$ leads to an abrupt change in p_h and the onset of spurious oscillations. A further reduction of

DOI: 10.1002/fld

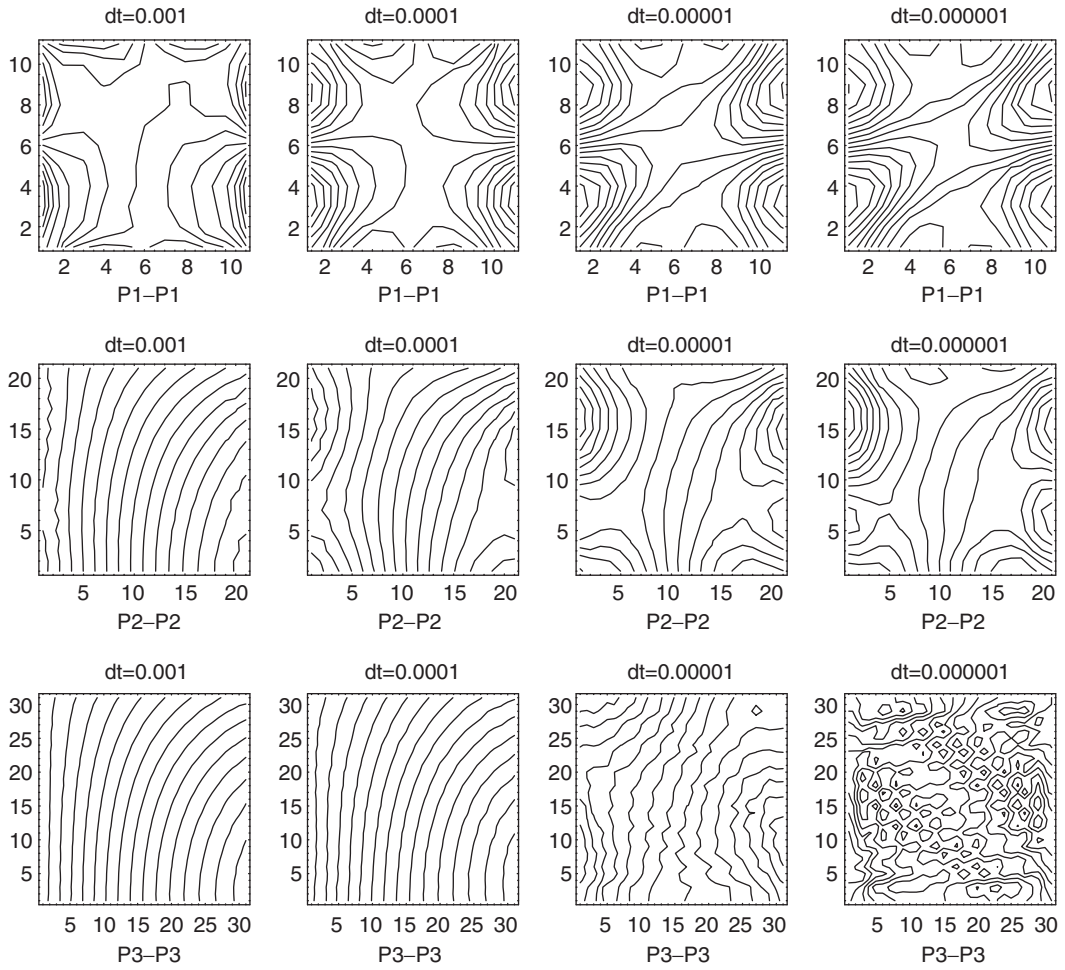

Figure 2. Pressure approximations in the $\Delta t \to 0$ limit; P1–P1, P2–P2, and P3–P3 stabilized methods with $\delta = 0.05$ and $n = 3, 4, 5, 6$. The tick marks denote node numbers in x (horizontal axis) and y (vertical axis) directions.

the time step to $(\Delta t)_6$ strengthens the oscillations and they assume a characteristic node-to-node pattern.

The sensitivity of the stabilized method with the P3–P3 element, compared to the relatively smooth transitions with the P1–P1 and P2–P2 pairs, calls for a further investigation. We first consider the behaviour of the method as δ changes. In Reference [3], it was established numerically that for $\gamma = 0$ method (8) remains stable for values of δ up to 100. For our study, we use the values $\delta = 5$, 0.5, 0.05, and 0.005 and then compute the finite element solution using the time steps $(\Delta t)_1$ and $(\Delta t)_6$. The first of these time steps satisfies $\Delta t > h^2$ and the top row in Figure 3 shows that in this case the only adverse effect from varying δ is the occurrence of small layers when $\delta = 5$. The condition $\Delta t > h^2$ does not hold for $(\Delta t)_6$. In this case, every change in δ causes an abrupt change

DOI: 10.1002/fld

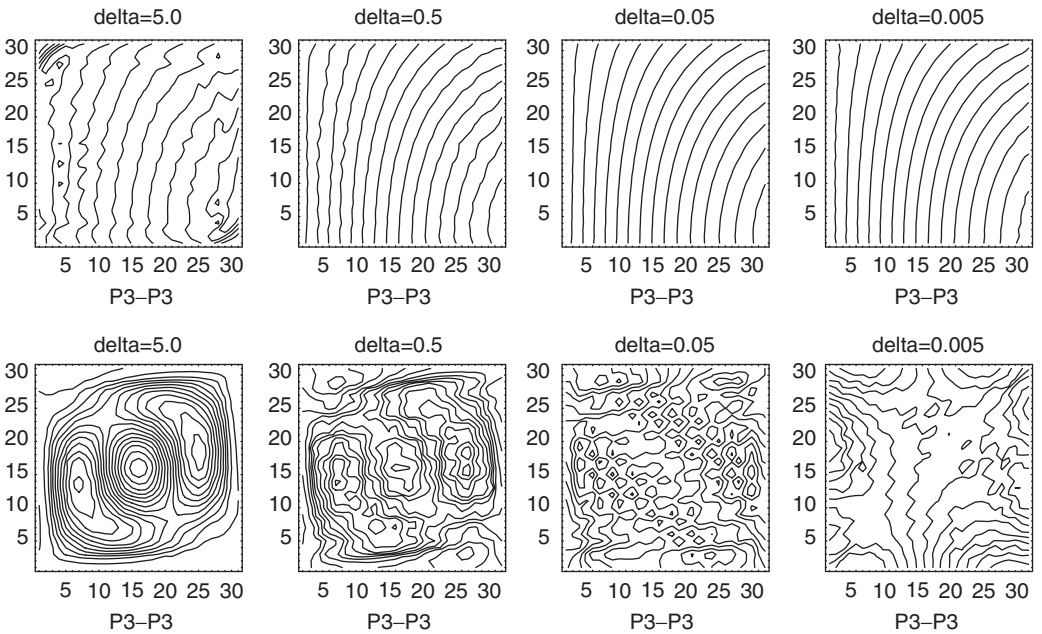

Figure 3. Pressure approximation: stabilized method with P3–P3 elements and $\delta = 5.0$, 0.5, 0.05, and 0.005. Top row: $\Delta t = (\Delta t)_1$; bottom row: $\Delta t = (\Delta t)_6$. The tick marks denote node numbers in x (horizontal axis) and y (vertical axis) directions.

in p_h. Note that the most oscillatory solutions occur for $\delta = 0.05$ (the optimal value) and $\delta = 0.5$, while $\delta = 5$, which was the worst value for $(\Delta t)_1$, yields an oscillation free (but completely wrong) pressure approximation.

We conclude the computational experiments by examining the effects of the quadrature rule on the P3–P3 pair. We take $\delta = 5$ and compute the approximate solution using $(\Delta t)_1$ and $(\Delta t)_6$. From the top row in Figure 4, we see that changing from a 7 point to a 13 point quadrature rule has no effect whatsoever for the larger time step. For $(\Delta t)_6$, we see that exactly the opposite is true. Using the less accurate 7 point rule leads to a perceptible change in p_h. While for both cases the approximate solutions are completely spurious, they look reasonably 'good' in the eyeball norm so that without knowledge of the exact solution, they could be easily mistaken for valid approximations. Repeating the same experiments with the P1–P1 and P2–P2 pairs shows less sensitivity with respect to the choice of δ and quadrature rule.

The following conclusions can be drawn from the computational experiments. For all three finite element spaces, the pressure approximations obtained using the stabilized method begin to deviate from the exact solution as the time step becomes smaller than h^2. Increasing the polynomial order makes the method more sensitive to changes in parameters and the pressure deviations become more pronounced. In contrast, the Taylor–Hood element pair remains remarkably stable in the $\Delta t \to 0$ limit. In the next section we show that the key to understanding this behaviour is the semi-discrete equation (18).

DOI: 10.1002/fld

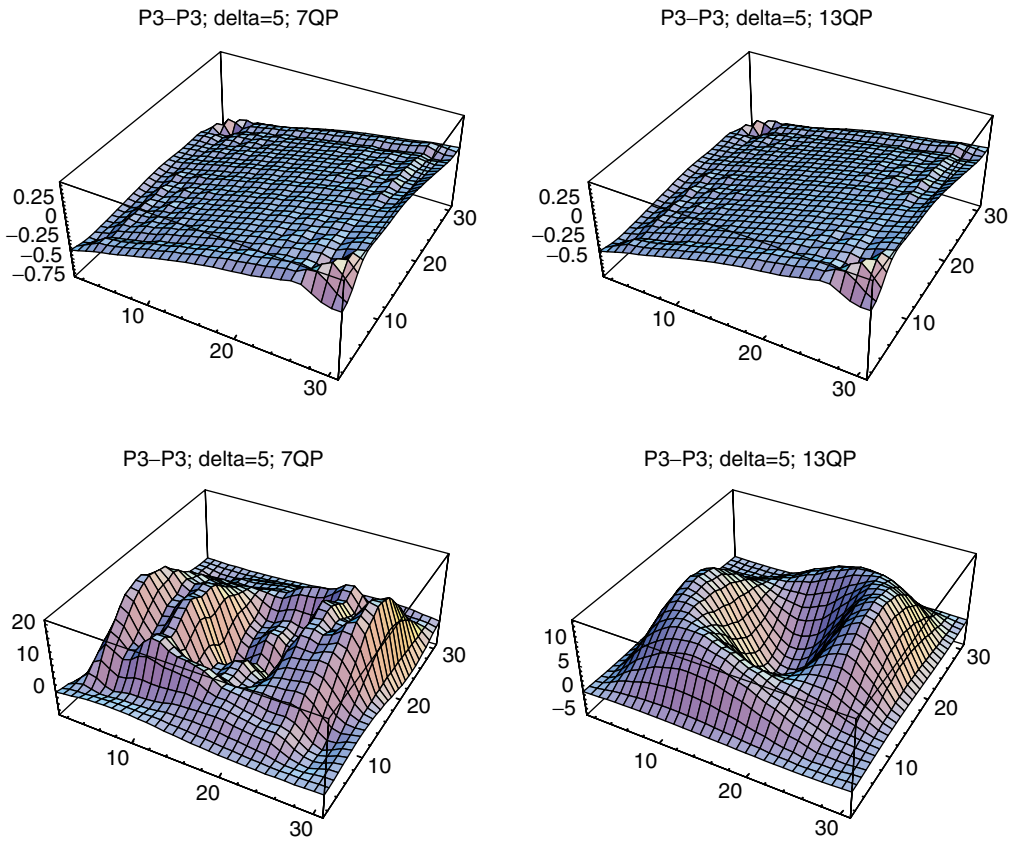

Figure 4. Pressure approximation: stabilized method with P3–P3 elements, $\delta = 5$, and different quadrature rule choices. Top row: $(\Delta t)_1$; bottom row: $(\Delta t)_6$.

5. ANALYSIS OF THE SEMI-DISCRETE PRESSURE OPERATOR

We examine the semi-discrete pressure operator for the case of $\gamma = 0$ in (18). This choice corresponds to the pressure-Poisson stabilized method, eliminates several unimportant terms, helps to avoid tedious calculations, and allows us to compare theory against the numerical data presented in Section 4. The cases $\gamma = 1$ and -1 will be considered briefly in Section 7.

We rewrite (18) in matrix form as

$$\begin{pmatrix} \mathbb{M}\dot{U} \\ \widetilde{\mathbb{B}}\dot{U} \end{pmatrix} + \begin{pmatrix} \mathbb{A} & \mathbb{B}^{\mathrm{T}} \\ -\mathbb{B} - \widetilde{\mathbb{S}} & \widetilde{\mathbb{K}} \end{pmatrix} \begin{pmatrix} U \\ P \end{pmatrix} = \begin{pmatrix} F \\ \widetilde{G} \end{pmatrix} \tag{23}$$

The second row in (23) is scaled by -1 to put the pressure equation in a canonical form that is shared with pressure-projection methods. The matrices $\mathbb{A}$, $\mathbb{B}$, and $\mathbb{M}$ were defined in (6) and (17)

DOI: 10.1002/fld

and the matrices

$$\widetilde{\mathbb{B}}_{ij} = \sum_{\mathscr{K} \in \mathscr{T}_h} \tau_{\mathscr{K}} (\boldsymbol{\xi}_j^h, \nabla \chi_i^h)_{\mathscr{K}}, \quad \widetilde{\mathbb{K}}_{ij} = \sum_{\mathscr{K} \in \mathscr{T}_h} \tau_{\mathscr{K}} (\nabla \chi_j^h, \nabla \chi_i^h)_{\mathscr{K}}, \quad \widetilde{\mathbb{S}}_{ij} = \sum_{\mathscr{K} \in \mathscr{T}_h} \tau_{\mathscr{K}} (\Delta \boldsymbol{\xi}_j^h, \nabla \chi_i^h)_{\mathscr{K}}$$

arise from the stabilizing term (21) and the consistency term (20). In addition, we have the stabilized source term

$$\widetilde{G}_i = \sum_{\mathscr{K} \in \mathscr{T}_h} \tau_{\mathscr{K}} (\mathbf{f}, \nabla \xi_i^h)_{\mathscr{K}}$$

Note that without stabilization, $\tau_{\mathscr{K}} = 0$ for all $\mathscr{K}$, all $\widetilde{(\cdot)}$ terms in (23) vanish, and the stabilized problem reduces to the mixed Galerkin semi-discrete equation (15). We remark that (15) is unstable for all equal order pairs considered in the experiments.

After $\dot{U}$ is eliminated from (23), we obtain the semi-discrete pressure equation

$$(\widetilde{\mathbb{K}} - \widetilde{\mathbb{B}} \mathbb{M}^{-1} \mathbb{B}^{\mathrm{T}}) P = \widetilde{G} - \widetilde{\mathbb{B}} \mathbb{M}^{-1} F + (\mathbb{B} + \widetilde{\mathbb{S}} + \widetilde{\mathbb{B}} \mathbb{M}^{-1} \mathbb{A}) U \tag{24}$$

To analyse (24) we assume that $\mathscr{T}_h$ is a regular triangulation. In this case $\tau_{\mathscr{K}}$ can be chosen to have the same value τ on all elements $\mathscr{K}$. This allows to simplify some 'broken' inner product terms of the type $\sum_{\mathscr{K} \in \mathscr{T}_h} \tau_{\mathscr{K}} (\cdot, \cdot)_{\mathscr{K}}$ to the standard L^2 inner product $\tau(\cdot, \cdot)$. Note that in this case $\widetilde{\mathbb{B}} = \tau \mathbb{B}$, $\widetilde{\mathbb{K}} = \tau \mathbb{K}$, $\widetilde{\mathbb{S}} = \tau \mathbb{S}$, and $\widetilde{G} = \tau G$, where $\mathbb{B}$ is the matrix defined in (6),

$$\mathbb{K}_{ij} = (\nabla \chi_j^h, \nabla \chi_i^h), \quad \mathbb{S}_{ij} = \sum_{\mathscr{K} \in \mathscr{T}_h} (\Delta \boldsymbol{\xi}_j^h, \nabla \chi_i^h)_{\mathscr{K}} \quad \text{and} \quad G_i = (\mathbf{f}, \nabla \xi_i^h) \tag{25}$$

With these assumptions the semi-discrete pressure equation (24) simplifies to

$$(\mathbb{K} - \mathbb{B} \mathbb{M}^{-1} \mathbb{B}^{\mathrm{T}}) P = G - \mathbb{B} \mathbb{M}^{-1} F + \left(\frac{1}{\tau} \mathbb{B} + \mathbb{S} + \mathbb{B} \mathbb{M}^{-1} \mathbb{A} \right) U \tag{26}$$

The matrix acting on the pressure can be viewed as a difference of two scaled discrete Laplacian operators. The same matrix difference arises in pressure-projection methods but there it acts to *relax* the continuity equation and provides additional stability that allows the use of equal-order interpolation [25]. The following theorem gives information about the eigenvalues of this matrix. In the theorem, $\|Q\|_{\mathbb{K}}^2 = Q^{\mathrm{T}} \mathbb{K} Q$.

Theorem 1

Let $\mathbb{B}$, $\mathbb{M}$, and $\mathbb{K}$ be defined as in (6), (17), and (25), respectively. Then,

$$Q^{\mathrm{T}} (\mathbb{K} - \mathbb{B} \mathbb{M}^{-1} \mathbb{B}^{\mathrm{T}}) Q \leqslant (1 - \mu_{\min}^2) \|Q\|_{\mathbb{K}}^2 \quad \forall Q \in (\mathrm{Ker}(\mathbb{B}^{\mathrm{T}}))^{\perp} \tag{27}$$

and

$$Q^{\mathrm{T}} (\mathbb{K} - \mathbb{B} \mathbb{M}^{-1} \mathbb{B}^{\mathrm{T}}) Q \geqslant (1 - \mu_{\max}^2) \|Q\|_{\mathbb{K}}^2 \quad \forall Q \in \mathbb{R}^M \tag{28}$$

where $\mu_{\min}^2 \neq 0$ and $\mu_{\max}^2$ are the smallest nonvanishing and the largest eigenvalues of the generalized eigenvalue problem

$$\mathbb{B} \mathbb{M}^{-1} \mathbb{B}^{\mathrm{T}} Q = \mathbb{K} Q \mu^2 \tag{29}$$

Moreover,

$$0 < \mu_{\min}^2 \leqslant \mu_{\max}^2 \leqslant 1 \tag{30}$$

DOI: 10.1002/fld

Note that there exist vectors $Q_{\min} \in \mathbb{R}^M$ and $Q_{\max} \in \mathbb{R}^M$ such that (27) and (28), respectively, hold with equality.

Proof
From (29), we have that

$$Q^{\mathrm{T}}(\mathbb{K} - \mathbb{B}\mathbb{M}^{-1}\mathbb{B}^{\mathrm{T}})Q = (1-\mu^2)Q^{\mathrm{T}}\mathbb{K}Q = (1-\mu^2)\|Q\|_{\mathbb{K}}^2 \tag{31}$$

A result in Reference [25, p. 22] proves that the matrix $\mathbb{K} - \mathbb{B}\mathbb{M}^{-1}\mathbb{B}^{\mathrm{T}}$ is positive semi-definite and hence (31) implies that $\mu^2 \leqslant 1$ for all eigenvalues μ^2 satisfying (29). This establishes the upper bound in (30). Furthermore, for any positive eigenvalue μ^2, we have that $0 < \mu_{\min}^2 \leqslant \mu^2 \leqslant \mu_{\max}^2 \leqslant 1$ so that $0 \leqslant 1-\mu_{\max}^2 \leqslant 1-\mu^2 \leqslant 1-\mu_{\min}^2 < 1$ and thus (27) and (28) follow from (31). Note that in (27) we restrict Q to belong to $(\mathrm{Ker}(\mathbb{B}^{\mathrm{T}}))^{\perp}$ because $Q \in \mathrm{Ker}(\mathbb{B}^{\mathrm{T}})$ are eigenvectors of (28) corresponding to the zero eigenvalue $\mu^2 = 0$.

Now, if we choose $Q_{\max} \in \mathbb{R}^M$ to be the generalized eigenvector satisfying $\mathbb{B}\mathbb{M}^{-1}\mathbb{B}^{\mathrm{T}}Q_{\max} = \mathbb{K}Q_{\max}\mu_{\max}^2$, then one easily sees that (28) holds with equality. Similarly, choosing $Q_{\min} \in \mathbb{R}^M$ such that $\mathbb{B}\mathbb{M}^{-1}\mathbb{B}^{\mathrm{T}}Q_{\min} = \mathbb{K}Q_{\min}\mu_{\min}^2$ leads to (27) holding with equality. □

This theorem refines the result proved in Reference [25]. As mentioned in our proof, the paper [25] established that $\mathbb{K} - \mathbb{B}\mathbb{M}^{-1}\mathbb{B}^{\mathrm{T}}$ is symmetric, positive semi-definite but did not provide bounds for the eigenvalues.

We will be interested in obtaining some information about $\mu_{\min}^2$ and especially about $\mu_{\max}^2$. To this end, we begin by noting that if $\mu^2 \neq 0$ and $Q \in (\mathrm{Ker}(\mathbb{B}^{\mathrm{T}}))^{\perp}$ are a generalized eigenpair for the problem (29), then there exists a $V \in (\mathrm{Ker}(\mathbb{B}))^{\perp}$ such that $\mu > 0$, Q, and V satisfy the generalized singular-value problem

$$\mathbb{B}^{\mathrm{T}}Q = \mathbb{M}V\mu \quad \text{and} \quad \mathbb{B}V = \mathbb{K}Q\mu \tag{32}$$

Indeed, if $\mu^2 \neq 0$ and $Q \in (\mathrm{Ker}(\mathbb{B}^{\mathrm{T}}))^{\perp}$ satisfy (29), then setting $\mu V = \mathbb{M}^{-1}\mathbb{B}^{\mathrm{T}}Q$ results in (32) and we are free to choose $\mu > 0$. Moreover, using (32), we have that $(\mathbb{B}V)^{\mathrm{T}}\mathbb{K}^{-1}(\mathbb{B}V) = (\mu\mathbb{K}Q)^{\mathrm{T}}\mathbb{K}^{-1}(\mu\mathbb{K}Q) = \mu^2 Q^{\mathrm{T}}\mathbb{K}Q \neq 0$ so that $\mathbb{B}V \neq 0$ and we can choose $V \in (\mathrm{Ker}(\mathbb{B}))^{\perp}$. See Reference [35] for more information on the existence of singular values and vectors and Reference [36, pp. 75–77] for a discussion of a similar singular-value problem arising from the inf–sup condition.

The minimum and maximum singular values of (32) may be characterized in terms of generalized Rayleigh quotients by the expressions

$$\mu_{\min} \equiv \min_{Q \in (\mathrm{Ker}(\mathbb{B}^{\mathrm{T}}))^{\perp}} \max_{V \in (\mathrm{Ker}(\mathbb{B}))^{\perp}} \frac{Q^{\mathrm{T}}\mathbb{B}V}{\|V\|_{\mathbb{M}}\|Q\|_{\mathbb{K}}} = \min_{Q \in (\mathrm{Ker}(\mathbb{B}^{\mathrm{T}}))^{\perp}} \max_{V \in \mathbf{R}^N} \frac{Q^{\mathrm{T}}\mathbb{B}V}{\|V\|_{\mathbb{M}}\|Q\|_{\mathbb{K}}} \tag{33}$$

and

$$\mu_{\max} \equiv \max_{Q \in (\mathrm{Ker}(\mathbb{B}^{\mathrm{T}}))^{\perp}} \max_{V \in (\mathrm{Ker}(\mathbb{B}))^{\perp}} \frac{Q^{\mathrm{T}}\mathbb{B}V}{\|V\|_{\mathbb{M}}\|Q\|_{\mathbb{K}}} = \max_{Q \in \mathbf{R}^M} \max_{V \in \mathbf{R}^N} \frac{Q^{\mathrm{T}}\mathbb{B}V}{\|V\|_{\mathbb{M}}\|Q\|_{\mathbb{K}}} \tag{34}$$

where $\|V\|_{\mathbb{M}}^2 = V^{\mathrm{T}}\mathbb{M}V$. In order to estimate the singular values we recast generalized Rayleigh quotients in (33) and (34) in terms of finite element functions. If $\mathbf{v}_h \in \mathscr{V}_h$ and $q_h \in \mathscr{P}_h$ are the finite element functions for which V and Q are the corresponding vector of coefficients, then,

DOI: 10.1002/fld

using the definitions of $\mathbb{M}$, $\mathbb{B}$, and $\mathbb{K}$, one can show that (33) and (34) are, respectively, equivalent to

$$\mu_{\min} = \inf_{q_h \in (\mathcal{N}^h)^\perp, q_h \neq 0} \sup_{\mathbf{v}_h \in \mathcal{V}_h, \mathbf{v}_h \neq \mathbf{0}} \frac{(\nabla q_h, \mathbf{v}_h)}{|q_h|_1 \|\mathbf{v}_h\|_0} \tag{35}$$

and

$$\mu_{\max} = \sup_{q_h \in \mathcal{P}_h, q_h \neq 0} \sup_{\mathbf{v}_h \in \mathcal{V}_h, \mathbf{v}_h \neq \mathbf{0}} \frac{(\nabla q_h, \mathbf{v}_h)}{|q_h|_1 \|\mathbf{v}_h\|_0} \tag{36}$$

where

$$\mathcal{N}^h = \{q_h \in \mathcal{P}_h \mid (\nabla q_h, \mathbf{v}_h) = 0 \quad \forall \mathbf{v}_h \in \mathcal{V}_h\}$$

i.e. $\mathcal{N}^h$ is the null space of the discrete gradient operator.

A few comments are now in order. The finite element expression (35) for the smallest singular value $\mu_{\min}$ resembles the inf–sup condition (7), but with 'reversed' norms applied to the velocity and pressure. In Reference [13, p. 273] this condition is referred to as the *alternative* inf–sup condition. The reversal of norms follows from the singular value decomposition (32) that was designed to provide bounds for the eigenvalues of $\mathbb{K} - \mathbb{B}\mathbb{M}^{-1}\mathbb{B}^{\mathrm{T}}$. Note also that if $(\mathcal{N}^h)^\perp = \mathbf{R}^M$, i.e. if the null space of the discrete gradient operator is trivial, then we have that $\mathbb{B}$ is of full row rank and (27) holds for all $Q \in \mathbf{R}^M$. Further discussion of the eigenvalue problem (29), relevant to the design of preconditioners for incompressible flows, can be found in Reference [13, p. 348]. Among other things, this discussion highlights some complications arising in the analysis of (29) in the case of natural outflow boundary conditions. However, these complications apply primarily to establishing the alternative inf–sup condition from (35).

We are, however, more interested in the lower bound (28) so that (36) is more relevant. From (28), we see that the stability of the semi-discrete pressure operator $\mathbb{K} - \mathbb{B}\mathbb{M}^{-1}\mathbb{B}^{\mathrm{T}}$ depends upon an *upper* bound for the *largest* singular value $\mu_{\max}$ instead of a *lower* bound for the *smallest* singular value $\mu_{\min}$; the latter is what one looks for when studying inf–sup conditions (again, see References [13, 36] for a discussion relevant to the inf–sup condition). Therefore, an immediate question raised by Theorem 1 is whether or not there exists a $\widehat{\mu}_{\max} < 1$ such that $\mu_{\max} \leqslant \widehat{\mu}_{\max}$ uniformly in $h > 0$? Our next result demonstrates that the answer to this question is negative.

Theorem 2
Let the hypothesis of Theorem 1 hold. If h denotes a characteristic mesh size, then

$$1 - \kappa h + O(h^2) \leqslant \mu_{\max} \leqslant 1 \quad \text{with } \kappa \geqslant 0 \tag{37}$$

where $\mu_{\max}$ is defined in (34).

Proof
The upper bound in (37) was proved in Theorem 1. For the lower bound, instead of giving a proof for general grids, we choose a setting that will allow us to compute explicitly the value of κ in (37). In doing so, we avoid tedious technical details and provide the reader with information about how the coercivity bound in (28) changes with the polynomial degree.

Let $\Omega = [0, 1]^2$ and Γ be its boundary. Consider partitions of Ω consisting of n^2 square elements. The side of each element has length $h = n^{-1}$. The value of κ will be calculated for equal-order

DOI: 10.1002/fld

bilinear, biquadratic, and bicubic finite element spaces. These spaces, denoted by Q_1–Q_1, Q_2–Q_2, and Q_3–Q_3, have 4, 9 and, 16 nodes per element, respectively. The standard nodal (Lagrangian) basis on Q_k is denoted by $\{\chi_i\}_{i=1}^{L}$. Therefore, if $N(\overline{\Omega})$ is the set of all grid nodes $\mathbf{x}_i$, then $\chi_i(\mathbf{x}_j)=\delta_{ij}$. The sets of all boundary nodes and all interior nodes are denoted by $N(\Gamma)$ and $N(\Omega)$, respectively; $\breve{\Omega}$ denotes the union of all interior elements, i.e. of those elements with vertices belonging to $N(\Omega)$; Ω_Γ is the complement of $\breve{\Omega}$.

The function

$$\widetilde{q}_h = x - \int_\Omega x \, \mathrm{d}\Omega$$

belongs to all $C^0(\Omega)$ piecewise polynomial spaces on a uniform square mesh and $\nabla\widetilde{q}_h=(1,0)^{\mathrm{T}}$. Define the velocity field $\widetilde{\mathbf{v}}_h$ by

$$\widetilde{\mathbf{v}}_h = \begin{pmatrix} \phi_h \\ 0 \end{pmatrix}, \quad \text{where } \phi_h(\mathbf{x}_i) = \begin{cases} 1 & \text{if } \mathbf{x}_i \in N(\Omega) \\ 0 & \text{if } \mathbf{x}_i \in N(\Gamma) \end{cases} \tag{38}$$

The function ϕ_h equals one on $\breve{\Omega}$ and transitions to 0 over Ω_Γ so that $\widetilde{\mathbf{v}}_h=0$ on $\partial\Omega$. We compute the fraction in (36) for the pair $(\widetilde{q}_h,\widetilde{\mathbf{v}}_h)$. The number of elements in Ω_Γ is $4(n-1)$ and the area of any element equals $n^{-2}=h^2$ so that the area of $\breve{\Omega}$ is $A(\breve{\Omega})=(1-4(n-1)/n^2)=(1-4h+4h^2)$. Therefore,

$$(\nabla\widetilde{q}_h,\widetilde{\mathbf{v}}_h) = \int_{\breve{\Omega}} 1 \, \mathrm{d}\Omega + \int_{\Omega_\Gamma} \phi_h \, \mathrm{d}\Omega = A(\breve{\Omega}) + \int_{\Omega_\Gamma} \phi_h \, \mathrm{d}\Omega = (1-4h+4h^2) + \int_{\Omega_\Gamma} \phi_h \, \mathrm{d}\Omega$$

$$\|\widetilde{\mathbf{v}}\|_0^2 = \int_{\breve{\Omega}} 1 \, \mathrm{d}\Omega + \int_{\Omega_\Gamma} \phi_h^2 \, \mathrm{d}\Omega = A(\breve{\Omega}) + \int_{\Omega_\Gamma} \phi_h^2 \, \mathrm{d}\Omega = (1-4h+4h^2) + \int_{\Omega_\Gamma} \phi_h^2 \, \mathrm{d}\Omega$$

and

$$|\widetilde{q}_h|_1^2 = \|\nabla\widetilde{q}_h\|_0^2 = \int_\Omega 1 \, \mathrm{d}\Omega = A(\Omega) = 1$$

The integrals of ϕ_h and ϕ_h^2 over Ω_Γ are easy to compute on the uniform mesh; Table I shows their values for the Q_1–Q_1, Q_2–Q_2, and Q_3–Q_3 element pairs. The values of $(\nabla\widetilde{q}_h,\widetilde{\mathbf{v}}_h)$ and $\|\widetilde{\mathbf{v}}_h\|_0^2$ are also given in Table I. The last row of that table provides asymptotic estimates for $\|\widetilde{\mathbf{v}}_h\|_0$.

Using the values in Table I, we determine that

$$\frac{(\nabla\widetilde{q}_h,\widetilde{\mathbf{v}}_h)}{|\widetilde{q}_h|_1\|\widetilde{\mathbf{v}}_h\|_0} = \frac{1-2h+h^2}{1-\frac{4}{3}h+O(h^2)} = 1-\frac{2}{3}h+O(h^2) \approx 1-0.66667h$$

for the Q_1–Q_1 element pair,

$$\frac{(\nabla\widetilde{q}_h,\widetilde{\mathbf{v}}_h)}{|\widetilde{q}_h|_1\|\widetilde{\mathbf{v}}_h\|_0} = \frac{1-\frac{2}{3}h+\frac{1}{9}h^2}{1-\frac{2}{5}h+O(h^2)} = 1-\frac{4}{15}h+O(h^2) \approx 1-0.26667h$$

DOI: 10.1002/fld

Table I. Integrals of ϕ_h and ϕ_h^2, $(\nabla\widetilde{q}_h, \widetilde{\mathbf{v}}_h)$, $\|\widetilde{\mathbf{v}}_h\|_0^2$, and asymptotic estimates for $\|\widetilde{\mathbf{v}}_h\|_0$ for uniform Q_1–Q_1, Q_2–Q_2, and Q_3–Q_3 element pairs.

	Q_1–Q_1	Q_2–Q_2	Q_3–Q_3
$\int_{\Omega_\Gamma} \phi_h \, \mathrm{d}\Omega$	$2h - 3h^2$	$\frac{10}{3}h - \frac{35}{9}h^2$	$\frac{7}{2}h - \frac{63}{16}h^2$
$\int_{\Omega_\Gamma} \phi_h^2 \, \mathrm{d}\Omega$	$\frac{4}{3}h - \frac{20}{9}h^2$	$\frac{16}{5}h - \frac{96}{5}h^2$	$\frac{347}{105}h - \frac{171071}{44100}h^2$
$(\nabla\widetilde{q}_h, \widetilde{\mathbf{v}}_h)$	$1 - 2h + h^2$	$1 - \frac{2}{3}h + \frac{1}{9}h^2$	$1 - \frac{1}{2}h + \frac{1}{16}h^2$
$\|\widetilde{\mathbf{v}}_h\|_0^2$	$1 - \frac{8}{3}h + \frac{16}{9}h^2$	$1 - \frac{4}{5}h + \frac{4}{25}h^2$	$1 - \frac{73}{105}h + \frac{5329}{44100}h^2$
$\|\widetilde{\mathbf{v}}_h\|_0 \approx$	$1 - \frac{4}{3}h + O(h^2)$	$1 - \frac{2}{5}h + O(h^2)$	$1 - \frac{73}{210}h + O(h^2)$

for the Q_2–Q_2 element pair, and

$$\frac{(\nabla\widetilde{q}_h, \widetilde{\mathbf{v}}_h)}{|\widetilde{q}_h|_1 \|\widetilde{\mathbf{v}}_h\|_0} = \frac{1 - \frac{1}{2}h + \frac{1}{16}h^2}{1 - \frac{73}{210}h + O(h^2)} = 1 - \frac{16}{105}h + O(h^2) \approx 1 - 0.15238h$$

for the Q_3–Q_3 element pair. With the obvious relation

$$\mu_{\max} = \sup_{q_h \in \mathscr{P}_h, q_h \neq 0} \sup_{\mathbf{v}_h \in \mathscr{V}_h, \mathbf{v}_h \neq \mathbf{0}} \frac{(\nabla q_h, \mathbf{v}_h)}{|q_h|_1 \|\mathbf{v}_h\|_0} \geqslant \frac{(\nabla\widetilde{q}_h, \widetilde{\mathbf{v}}_h)}{|\widetilde{q}_h|_1 \|\widetilde{\mathbf{v}}_h\|_0}$$

we obtain the lower bound in (37) with

$$\kappa = \begin{cases} \frac{2}{3} & \text{for the } Q_1\text{–}Q_1 \text{ element pair} \\ \frac{4}{15} & \text{for the } Q_2\text{–}Q_2 \text{ element pair} \\ \frac{16}{105} & \text{for the } Q_3\text{–}Q_3 \text{ element pair} \end{cases} \tag{39}$$

□

The following result is an immediate consequence of Theorems 1 and 2.

Corollary 3
Let the hypothesis of Theorem 1 hold. Then, there exists a $Q_{\max} \in \mathbf{R}^M$ such that

$$Q_{\max}^{\mathrm{T}}(\mathbb{K} - \mathbb{B}\mathbb{M}^{-1}\mathbb{B}^{\mathrm{T}}) Q_{\max} \leqslant (2\kappa h + O(h^2)) \| Q_{\max} \|_{\mathbb{K}}^2 \tag{40}$$

where $\kappa > 0$ is given in (39).

Proof
From Theorem 1, there exists a $Q_{\max} \in \mathbf{R}^M$ such that

$$Q_{\max}^{\mathrm{T}}(\mathbb{K} - \mathbb{B}\mathbb{M}^{-1}\mathbb{B}^{\mathrm{T}}) Q_{\max} = (1 - \mu_{\max}^2) \| Q_{\max} \|_{\mathbb{K}}^2$$

From (37), we have that

$$1 - \mu_{\max}^2 \leqslant 2\kappa h + O(h^2)$$

Combining these two results yields (40). □

DOI: 10.1002/fld

Corollary 3 shows that for sufficiently fine uniform square grids

$$Q_{\max}^{\mathrm{T}}(\mathbb{K}-\mathbb{B}\mathbb{M}^{-1}\mathbb{B}^{\mathrm{T}})Q_{\max}\leqslant\|Q_{\max}\|_{\mathbb{K}}^{2}\begin{cases}\frac{4}{3}h+O(h^{2}) & \text{for the } Q_1\text{–}Q_1 \text{ element pair}\\ \frac{8}{15}h+O(h^{2}) & \text{for the } Q_2\text{–}Q_2 \text{ element pair}\\ \frac{32}{105}h+O(h^{2}) & \text{for the } Q_3\text{–}Q_3 \text{ element pair}\end{cases}$$

so that $\mathbb{K}-\mathbb{B}\mathbb{M}^{-1}\mathbb{B}^{\mathrm{T}}$ is not uniformly invertible. Seemingly, raising the polynomial degree by one roughly halves the constant κ. Thus, for higher-order element pairs, the pressure operator $\mathbb{K}-\mathbb{B}\mathbb{M}^{-1}\mathbb{B}^{\mathrm{T}}$ will become computationally unstable for coarser grids. This finding is confirmed by our experiments. From the experiments we also see that the spurious modes of the semi-discrete pressure operator lack an obvious pattern that makes their potential identification and elimination extremely difficult. Specifically, these unstable modes are not necessarily associated with a node-to-node checkerboard like oscillation even on a uniform grid.

6. THE STABILIZING ROLE OF TIME DISCRETIZATION

The results of Section 5 show that the semi-discrete pressure operator $\mathbb{K}-\mathbb{B}\mathbb{M}^{-1}\mathbb{B}^{\mathrm{T}}$ obtained with $\gamma=0$ is unstable. In this section, we show that the backward-Euler implicit time discretization contributes stabilizing terms that can render the fully discrete pressure operator stable. However, this stabilization is conditional and requires a sufficiently large time step. If the time step is too small, the stabilization provided by the implicit time discretization is not sufficient to overcome the instability of the semi-discrete operator. Our analysis applies to other implicit time discretization methods, e.g. the generalized trapezoidal rule, because they contribute similar stabilization terms to the fully discrete pressure operator; see Reference [18].

Assuming the simplifications introduced in Section 5, the application of the backward-Euler rule to (23) results in the fully discrete formulation

$$\begin{pmatrix}\mathbb{M}+\Delta t\mathbb{A} & \Delta t\mathbb{B}^{\mathrm{T}}\\ (\tau-\Delta t)\mathbb{B}-\tau\Delta t\mathbb{S} & \tau\Delta t\mathbb{K}\end{pmatrix}\begin{pmatrix}U^{k+1}\\ P^{k+1}\end{pmatrix}=\begin{pmatrix}\mathbb{M} & 0\\ \tau\mathbb{B} & 0\end{pmatrix}\begin{pmatrix}U^{k}\\ P^{k}\end{pmatrix}+\Delta t\begin{pmatrix}F^{k+1}\\ \tau G^{k+1}\end{pmatrix}\tag{41}$$

where the superscripts $k+1$ and k refer to values at time steps t_{k+1} and t_k, respectively. A simple but tedious calculation [18] shows that

$$\begin{aligned}U^{k+1}=&(\mathbb{M}+\Delta t\mathbb{A})^{-1}[\mathbb{M}-\mathbb{B}^{\mathrm{T}}(\mathbb{K}+\mathbb{N}\mathbb{B}^{\mathrm{T}})^{-1}(\mathbb{N}\mathbb{M}+\mathbb{B})]U^{k}\\ &+\Delta t(\mathbb{M}+\Delta t\mathbb{A})^{-1}[F^{k+1}-\mathbb{B}^{\mathrm{T}}(\mathbb{K}+\mathbb{N}\mathbb{B}^{\mathrm{T}})^{-1}(\mathbb{N}F^{k+1}+G^{k+1})]\end{aligned}\tag{42}$$

for the velocity and

$$P^{k+1}=(\mathbb{K}+\mathbb{N}\mathbb{B}^{\mathrm{T}})^{-1}\left[\frac{1}{\Delta t}(\mathbb{N}\mathbb{M}+\mathbb{B})U^{k}+\mathbb{N}F^{k+1}+G^{k+1}\right]\tag{43}$$

for the pressure, where

$$\mathbb{N}=\left(\frac{\Delta t}{\tau}\mathbb{B}-\mathbb{B}+\Delta t\mathbb{S}\right)(\mathbb{M}+\Delta t\mathbb{A})^{-1}$$

DOI: 10.1002/fld

The symmetric, positive definite matrices $\mathbb{M}$ and $\mathbb{A}$ are invertible for any standard choice of finite element approximating spaces for the velocity. As a result, the matrix $\mathbb{M}+\Delta t\,\mathbb{A}$ is likewise invertible. Therefore, the well posedness of solutions (42) and (43) is dependent upon the invertibility of the fully discrete pressure operator $\mathbb{K}+\mathbb{N}\mathbb{B}^{\mathrm{T}}$. The following theorem shows that this operator is conditionally stable. We first remark, however, that although the term $1/\Delta t(\mathbb{N}\mathbb{M}+\mathbb{B})$ on the right-hand side of (43) may appear to be a potential source of instability, in fact, that term is benign.

Theorem 4
The fully discrete pressure operator $\mathbb{K}+\mathbb{N}\mathbb{B}^{\mathrm{T}}$ satisfies

$$Q^{\mathrm{T}}(\mathbb{K}+\mathbb{N}\mathbb{B}^{\mathrm{T}})Q = Q^{\mathrm{T}}\left(\mathbb{K}+\left(\frac{\Delta t}{\tau}-1\right)(\mathbb{B}\mathbb{M}^{-1}\mathbb{B}^{\mathrm{T}}+O(\Delta t))\right)Q+O(\Delta t) \tag{44}$$

and, for any $\alpha>0$,

$$Q^{\mathrm{T}}(\mathbb{K}+\mathbb{N}\mathbb{B}^{\mathrm{T}})Q\geqslant\frac{1}{2}\min\{1,\alpha\}\|Q\|_{\mathbb{K}}^2 \quad \text{if } \frac{\Delta t}{\tau}\geqslant\alpha \tag{45}$$

Proof
Substituting for $\mathbb{N}$, the fully discrete pressure operator takes the form

$$\mathbb{K}+\mathbb{N}\mathbb{B}^{\mathrm{T}}=\left(\mathbb{K}+\left(\frac{\Delta t}{\tau}-1\right)\mathbb{B}(\mathbb{M}+\Delta t\,\mathbb{A})^{-1}\mathbb{B}^{\mathrm{T}}\right)+\Delta t\,\mathbb{S}(\mathbb{M}+\Delta t\,\mathbb{A})^{-1}\mathbb{B}^{\mathrm{T}} \tag{46}$$

The term $\mathbb{S}(\mathbb{M}+\Delta t\,\mathbb{A})^{-1}\mathbb{B}^{\mathrm{T}}$ is a non-symmetric discretization of $-\Delta^2$ (a negative semi-definite operator) and does not provide stabilization. Because in (46) this term is multiplied by Δt, it may be neglected compared to $\mathbb{B}(\mathbb{M}+\Delta t\,\mathbb{A})^{-1}\mathbb{B}^{\mathrm{T}}$. Therefore, from (46), we obtain (44).

The matrix $\mathbb{B}\mathbb{M}^{-1}\mathbb{B}^{\mathrm{T}}$ is at least positive semi-definite so that if $\alpha\geqslant1$, i.e. if $\Delta t/\tau\geqslant1$, we have from (44) that for some σ

$$Q^{\mathrm{T}}(\mathbb{K}+\mathbb{N}\mathbb{B}^{\mathrm{T}})Q\geqslant Q^{\mathrm{T}}\mathbb{K}Q+O(\Delta t)\geqslant(1-\sigma\Delta t)\|Q\|_{\mathbb{K}}^2\geqslant\tfrac{1}{2}\|Q\|_{\mathbb{K}}^2=\tfrac{1}{2}\min\{1,\alpha\}\|Q\|_{\mathbb{K}}^2$$

so that (45) holds for Δt small enough with $\Delta t/\tau\geqslant\alpha$ with $\alpha\geqslant1$.

Now, as for (28), we can show from (44) that if $\Delta t/\tau<1$, then

$$Q^{\mathrm{T}}(\mathbb{K}+\mathbb{N}\mathbb{B}^{\mathrm{T}})Q\geqslant\left(1+\left(\frac{\Delta t}{\tau}-1\right)\mu_{\max}^2+O(\Delta t)\right)\|Q\|_{\mathbb{K}}^2+O(\Delta t) \tag{47}$$

If also $\Delta t/\tau\geqslant\alpha$ with now $\alpha<1$, we have from (47) and $\mu_{\max}^2\leqslant1$ that

$$Q^{\mathrm{T}}(\mathbb{K}+\mathbb{N}\mathbb{B}^{\mathrm{T}})Q\geqslant(\alpha+O(\Delta t))\|Q\|_{\mathbb{K}}^2+O(\Delta t)\geqslant\frac{\alpha}{2}\|Q\|_{\mathbb{K}}^2=\frac{1}{2}\min\{1,\alpha\}\|Q\|_{\mathbb{K}}^2 \tag{48}$$

so that (45) holds for Δt small enough with $\Delta t/\tau\geqslant\alpha$ with $\alpha<1$. □

Theorem 4 has the following obvious implications for the fully discrete pressure operator $\mathbb{K}+\mathbb{N}\mathbb{B}^{\mathrm{T}}$.

Corollary 5
If $\Delta t/\tau\geqslant\alpha$, where the value of α is independent of h and Δt, then the fully discrete pressure operator $\mathbb{K}+\mathbb{N}\mathbb{B}^{\mathrm{T}}$ is uniformly coercive.

DOI: 10.1002/fld

On the other hand,

$$\mathbb{K} + \mathbb{N}\mathbb{B}^{\mathrm{T}} \to \mathbb{K} - \mathbb{B}\mathbb{M}^{-1}\mathbb{B}^{\mathrm{T}} \quad \text{uniformly in } h \text{ if } \frac{\Delta t}{\tau} \to 0 \quad \text{as } \Delta t \to 0 \tag{49}$$

i.e. the fully discrete pressure operator reduces to the semi-discrete pressure operator $\mathbb{K}-\mathbb{B}\mathbb{M}^{-1}\mathbb{B}^{\mathrm{T}}$.

Proof
The uniform coercivity of $\mathbb{K}+\mathbb{N}\mathbb{B}^{\mathrm{T}}$ in case the value of α is independent of h and Δt is an obvious consequence of (45). Also, (49) follows easily from (44). □

From (44) we see that implicit time discretization contributes the stabilizing term $(\Delta t/\tau)\mathbb{B}\mathbb{M}^{-1}\mathbb{B}^{\mathrm{T}}$ to the fully discrete pressure operator. If $\Delta t/\tau \geqslant \alpha$ with α fixed, this term is sufficient to overcome the destabilizing term $\mathbb{B}\mathbb{M}^{-1}\mathbb{B}^{\mathrm{T}}$ appearing in the semi-discrete pressure operator. However, if $\Delta t/\tau \to 0$, the stabilization term disappears and we are left with the semi-discrete pressure operator $\mathbb{K} - \mathbb{B}\mathbb{M}^{-1}\mathbb{B}^{\mathrm{T}}$ that, according to Corollary 3, is unstable for equal-order interpolation.

The latter happens for the spatial τ (10) when $\Delta t \to 0$ and h is held fixed. This explains the onset of numerical difficulties with the pressure as Δt becomes small in our computational experiments. Therefore, to avoid the small time step instability when using the spatial τ it is necessary to refine h simultaneously with Δt so as to ensure that $\Delta t/(\delta h^2) > \alpha$ for some positive α that is independent of both Δt and h. The results (45) and (49), respectively, show that in this case the fully discrete pressure operator $\mathbb{K} + \mathbb{N}\mathbb{B}^{\mathrm{T}}$ is stable. Note that from (42)

$$U^{k+1} = U^k + O(\Delta t)$$

This indicates that as $\Delta t \to 0$ with h fixed in (10), the velocity approximations are stable, i.e. $U^{k+1} \to U^k$ as $\Delta t \to 0$. Computational experiments show that this is indeed the case. However, while the stability of the velocity does not seem to be affected, the problems with the pressure operator may still be relevant to the accuracy of those approximations.

We also note that for the transient τ defined in (19)

$$\tau = \frac{\Delta t}{2}\left(1 + \left(\frac{\Delta t}{\delta h^2}\right)^2\right)^{-1/2}$$

and so, for h fixed and $\Delta t \to 0$ it follows that $\Delta t/\tau > 2$. While this seems to suggest that the transient τ will avoid the small time step instability, the problem is that in the small time step limit $\tau = O(\Delta t)$ and all stabilizing terms in (41) become negligible. As a result, this problem defaults to an unstable discretization of (15).

Therefore, we see that in the small time step limit, the definition of τ is subject to two competing constraints. On one hand, to stabilize the velocity–pressure pair τ must scale as $O(h^2)$. On the other hand, to ensure that $\Delta t/\tau > \alpha$ the stabilizing parameter must scale as $O(\Delta t)$. These constraints are impossible to satisfy if Δt and h are allowed to vary independently of each other. In particular, in the small time step limit the spatial discretization step h must *necessarily* decrease as $\Delta t \to 0$.

7. SEMI-DISCRETE PRESSURE OPERATOR FOR $\gamma \neq 0$

The analyses of Sections 5 and 6 addressed the pressure-Poisson stabilized Galerkin method for which $\gamma = 0$ in (9). Our main results show that for $\gamma = 0$ the semi-discrete stabilized Stokes

DOI: 10.1002/fld

equations (18) give rise to an unstable pressure operator and that the associated fully discrete pressure operator becomes unstable in the small time step limit. In this section we extend these results to Galerkin-least-squares ($\gamma = 1$) and the Douglas–Wang ($\gamma = -1$) stabilization methods with the spatial definition (10) of τ. Assuming that $\tau_{\mathscr{K}} = \tau = \delta h^2$ the modified semi-discrete equation (18) is

$$\begin{pmatrix} (\mathbb{M} + \gamma\tau\mathbb{C})\,\dot{U} \\ \tau\mathbb{B}\,\dot{U} \end{pmatrix} + \begin{pmatrix} \mathbb{A} - \gamma\tau\mathbb{D} & \mathbb{B}^{\mathrm{T}} + \gamma\tau\mathbb{S}^{\mathrm{T}} \\ -\mathbb{B} - \tau\mathbb{S} & \tau\mathbb{K} \end{pmatrix} \begin{pmatrix} U \\ P \end{pmatrix} = \begin{pmatrix} F + \gamma\tau H \\ \tau G \end{pmatrix} \tag{50}$$

The matrices $\mathbb{M}$, $\mathbb{A}$, $\mathbb{B}$, $\mathbb{K}$ and $\mathbb{S}$ have already been described;

$$\mathbb{C}_{ij} = \tau \sum_{\mathscr{K} \in \mathscr{T}_h} (\boldsymbol{\xi}_j^h, \Delta\boldsymbol{\xi}_i^h)_{\mathscr{K}}; \quad \mathbb{D}_{ij} = \tau \sum_{\mathscr{K} \in \mathscr{T}_h} (\Delta\boldsymbol{\xi}_j^h, \Delta\boldsymbol{\xi}_i^h)_{\mathscr{K}} \quad \text{and} \quad (H)_i = \tau \sum_{\mathscr{K} \in \mathscr{T}_h} (\mathbf{f}, \Delta\boldsymbol{\xi}_i^h)_{\mathscr{K}}$$

We note that $\mathbb{S}$, $\mathbb{C}$, $\mathbb{D}$ and H vanish for piecewise linear finite elements and (50) defaults to the same penalty-like formulation for all values of γ. Therefore, we assume that $\mathscr{V}_h$ and $\mathscr{P}_h$ are at least quadratic (or biquadratic) spaces.

A minimal condition for the solvability of (50) (or (18)) is that the matrix $\mathbb{M} + \gamma\tau\mathbb{C}$ is invertible. Recall that the value of δ may be restricted to guarantee stability of the steady-state problem (8). The following lemma shows that δ may have to be further restricted in order to ensure that $(\mathbb{M} + \gamma\tau\mathbb{C})^{-1}$ exists. To state the lemma we recall the inverse inequality [1]

$$\|\Delta\mathbf{u}_h\|_{0,\mathscr{K}} \leqslant h^{-2} C_I \|\mathbf{u}_h\|_{0,\mathscr{K}}$$

Lemma 6
For any $U \in \mathbf{R}^N$ we have that

$$(1 - \delta C_I) U^{\mathrm{T}} \mathbb{M} U \leqslant U^{\mathrm{T}} (\mathbb{M} + \gamma\tau\mathbb{C}) U \leqslant (1 + \delta C_I) U^{\mathrm{T}} \mathbb{M} U \tag{51}$$

If $\delta < C_I^{-1}$ then, the matrix $\mathbb{M} + \gamma\tau\mathbb{C}$ is invertible.

Proof
Definition of $\mathbb{M}$ and $\mathbb{C}$ gives

$$U^{\mathrm{T}} (\mathbb{M} + \gamma\tau\mathbb{C}) U = \|\mathbf{u}_h\|_0^2 + \gamma\tau \sum_{\mathscr{K} \in \mathscr{T}_h} (\mathbf{u}_h, \Delta\mathbf{u}_h)_{\mathscr{K}}$$

Using the Cauchy inequality, the inverse inequality and that $\tau = \delta h^2$

$$\tau \sum_{\mathscr{K} \in \mathscr{T}_h} (\mathbf{u}_h, \Delta\mathbf{u}_h)_{\mathscr{K}} \leqslant \delta C_I \|\mathbf{u}_h\|_0^2$$

Using again that $\|\mathbf{u}_h\|_0^2 = U^{\mathrm{T}} \mathbb{M} U$ gives (51). If $\delta < C_I^{-1}$ the lower bound in (51) implies that $\mathbb{M} + \gamma\tau\mathbb{C}$ is coercive and hence, invertible. □

Assuming that $\delta < C_I^{-1}$, so that $\mathbb{M} + \gamma\tau\mathbb{C}$ is invertible, the general form of the semi-discrete pressure equation (24) with $\gamma \neq 0$ is given by

$$\begin{aligned} &(\mathbb{K} - \mathbb{B}(\mathbb{M} + \gamma\tau\mathbb{C})^{-1}(\mathbb{B} + \gamma\tau\mathbb{S})^{\mathrm{T}})\,P \\ &\quad = G - \mathbb{B}(\mathbb{M} + \gamma\tau\mathbb{C})^{-1}(F + \gamma\tau H) + (\tau^{-1}\mathbb{B} + \tau\mathbb{S} + \mathbb{B}(\mathbb{M} + \gamma\tau\mathbb{C})^{-1}\mathbb{A} - \gamma\mathbb{D})U \end{aligned} \tag{52}$$

DOI: 10.1002/fld

From (51) it follows that $\mathbb{M}+\gamma\tau\mathbb{C}$ is spectrally equivalent to $\mathbb{M}$, and from (25) and the inverse inequality we see that $\tau\mathbb{S}$ is of the same order as $\mathbb{B}$. Therefore, spectrally

$$\mathbb{K}-\mathbb{B}(\mathbb{M}+\gamma\tau\mathbb{C})^{-1}(\mathbb{B}+\gamma\tau\mathbb{S})^{\mathrm{T}}\sim\mathbb{K}-\mathbb{B}\mathbb{M}^{-1}\mathbb{B}$$

As a result, the Galerkin-least-squares ($\gamma=1$) and the Douglas–Wang ($\gamma=-1$) semi-discrete pressure operators are qualitatively equivalent to the pressure-Poisson ($\gamma=0$) semi-discrete operator. The instability of the Galerkin-least-squares and the Douglas–Wang semi-discrete pressure operators has the same implications on the fully discrete pressure operators for those methods as were discussed in Section 6 for the pressure-Poisson fully discrete pressure operator. In particular, for all three methods, the fully discrete pressure operator is unstable in the small time-step limit. This is the main result of our paper.

8. CONNECTION WITH PRESSURE-PROJECTION METHODS

An interesting observation is that the operator $\mathbb{K}-\mathbb{B}\mathbb{M}^{-1}\mathbb{B}^{\mathrm{T}}$ also arises in pressure-projection methods. The main difference with (24) is how $\mathbb{K}-\mathbb{B}\mathbb{M}^{-1}\mathbb{B}^{\mathrm{T}}$ enters that formulation. In a pressure-projection method, this matrix effectively relaxes the discretized continuity equation [25] to

$$-\mathbb{B}U+\Delta t(\mathbb{K}-\mathbb{B}\mathbb{M}^{-1}\mathbb{B}^{\mathrm{T}})P=0 \tag{53}$$

while the pressure operator is still given by the symmetric and positive definite stiffness matrix $\mathbb{K}$. In contrast, in (24), the matrix $\mathbb{K}-\mathbb{B}\mathbb{M}^{-1}\mathbb{B}^{\mathrm{T}}$ *is the pressure operator* itself. To stabilize (53), $\mathbb{K}-\mathbb{B}\mathbb{M}^{-1}\mathbb{B}^{\mathrm{T}}$ only has to be positive semi-definite, whereas to provide a well-posed semi-discrete equation (24), this matrix needs to be uniformly (in h) positive definite.

A pressure-projection method implemented with equal-order finite element spaces will also become unstable when Δt is small relative to h^2. However, the cause of this instability is fundamentally different from the one in stabilized methods. In the latter setting, the instability is caused by the fact that the fully discrete pressure operator approaches the unstable semi-discrete pressure operator $\mathbb{K}-\mathbb{B}\mathbb{M}^{-1}\mathbb{B}^{\mathrm{T}}$. In contrast, in a pressure-projection method the instability arises from the insufficient amount of stabilization provided by $\Delta t(\mathbb{K}-\mathbb{B}\mathbb{M}^{-1}\mathbb{B}^{\mathrm{T}})$ for small Δt.

9. CONCLUDING REMARKS

The main result of this paper is that a method of lines approach in conjunction with residual based stabilization for the spatial discretization of unsteady incompressible flow problems leads to an unstable semi-discrete pressure operator. The backward-Euler time discretization method contributes terms that stabilize this operator, provided[‖] $\Delta t/\tau\geqslant\alpha$ for α independent of h and Δt, i.e. the fully discrete equations are conditionally stable. This can be seen as a consequence of the fact that as $\Delta t\to 0$, the fully discrete problem converges to the (unstable) semi-discrete formulation.

[‖] This lower bound on the ratio $\Delta t/h^2$, associated with the spatial τ, should be contrasted with the classical stability condition for the *explicit* forward-Euler scheme that involves and *upper bound* on that ratio.

DOI: 10.1002/fld

Theoretical estimates indicate that the onset of numerical instabilities is faster and more severe for higher polynomial degrees. These findings are confirmed by computational experiments.

Our analysis shows that the small time-step instability is inherent to the combination of *residual-based* stabilization in space and *implicit integration* in time. This conclusion can be elucidated by using variational multiscale analysis (VMS) [37] ideas. Specifically, VMS shows that residual stabilization is equivalent to a subgrid model and adds stability by approximating the unresolved scales. As a result, a proper approach to stabilize an unsteady problem requires subgrid models that approximate unresolved scales both in *space and time*. However, a method of lines approach separates the discretization steps. As a result, extension of stabilized methods formulated for steady flows fails to account for the unresolved temporal scales.

The problems and issues discussed in this paper are typical only for the small time-step limit. For standard incompressible flow applications where small time-steps are not needed, the use of consistent spatial stabilization, in conjunction with an implicit time integration, remains an attractive and viable alternative to mixed Galerkin methods. This is particularly true if the main goal of the simulation is to compute a steady-state solution. However, for applications that require small time-steps, such as chemically reacting flows, one has to exercise extreme caution when the time-step is less than $O(h^2)$. For such applications we recommend that $\Delta t/\delta h^2 > \alpha$ for some fixed positive α. Corollary 5 asserts that in this case the fully discrete pressure operator will be uniformly coercive, and so, using a small α gives more flexibility in the choice of Δt. Another alternative is to use nonresidual stabilized methods such as pressure projection [5, 38, 39], or pressure jump [40, 41] stabilized methods, or a stable mixed method. It may also be possible to avoid the small time step instability by using a space–time stabilized formulation [42]. However, further studies of such methods will be needed before a conclusion can be made about their stability in the small time step limit.

ACKNOWLEDGEMENTS

Theorem 1 was inspired by Stoyan's result in Reference [43]. John Shadid called our attention to the small time step instabilities and offered useful insight into the application settings where they arise. Marek Behr confirmed some of our numerical results. Isaak Harari drew our attention to Reference [24] and the small time step issues in parabolic problems. We thank Tom Hughes, Guglielmo Scovazzi and Scott Collis for helpful discussions on the small time step instability raised by our analysis. We also thank the anonymous referees for the careful reading of the manuscript and for pointing out References [22, 23].

Sandia is a multiprogram laboratory operated by Sandia Corporation, a Lockheed-Martin Company, for the U.S. Department of Energy's National Nuclear Security Administration under contract DE-AC-94AL85000. The work of M. Gunzburger was supported in part by the Computer Science Research Institute, Sandia National Laboratories, under contract 18407.

REFERENCES

1. Girault V, Raviart P. *Finite Element Methods for Navier–Stokes Equations*. Springer: Berlin, 1986.
2. Gunzburger M. *Finite Element Methods for Viscous Incompressible Flows*. Academic: Boston, 1989.
3. Barth T, Bochev P, Gunzburger M, Shadid JN. A taxonomy of consistently stabilized finite element methods for the Stokes problem. *SIAM Journal on Scientific Computing* 2004; **25**:1585–1607.
4. Behr MA, Franca LP, Tezduyar TE. Stabilized finite element methods for the velocity–pressure-stress formulation of incompressible flows. *Computer Methods in Applied Mechanics and Engineering* 1993; **104**:31–48.
5. Bochev P, Gunzburger M. An absolutely stable pressure-Poisson stabilized method for the Stokes equations. *SIAM Journal on Numerical Analysis* 2005; **42**(3):1189–1207.
6. Brezzi F, Douglas J. Stabilized mixed methods for the Stokes problem. *Numerische Mathematik* 1988; **53**:225–235.

DOI: 10.1002/fld

7. Douglas J, Wang J. An absolutely stabilized finite element method for the Stokes problem. *Mathematics of Computation* 1989; **52**:495–508.
8. Franca L, Hughes TJR, Stenberg R. Stabilized finite element methods. In *Incompressible Computational Fluid Dynamics*, Gunzburger M, Nicolaides R (eds). Cambridge University Press: Cambridge, MA, 1993; 87–108.
9. Hughes TJR, Franca LP, Hulbert G. A new finite element formulation for computational fluid dynamics: VIII. The Galerkin/least-squares method for advective–diffusive equations. *Computer Methods in Applied Mechanics and Engineering* 1989; **73**:173–189.
10. Hughes TJR, Franca L. A new finite element formulation for computational fluid dynamics: VII. The Stokes problem with various well-posed boundary conditions: symmetric formulations that converge for all velocity pressure spaces. *Computer Methods in Applied Mechanics and Engineering* 1987; **65**:85–96.
11. Hughes TJR, Franca L, Balestra M. A new finite element formulation for computational fluid dynamics: circumventing the Babuska–Brezzi condition: a stable Petrov–Galerkin formulation of the Stokes problem accommodating equal-order interpolations. *Computer Methods in Applied Mechanics and Engineering* 1986; **59**:85–99.
12. Baiocchi C, Brezzi F. Stabilization of unstable numerical methods. In *Proceedings of the Problemi attuali dell' analisi e della fisica matematica*, Taormina, 1992; 59–64.
13. Elman HC, Silvester DJ, Wathen AJ. Finite elements and fast iterative solvers with applications in incompressible fluid dynamics. *Numerical Mathematics and Scientific Computation*. Oxford University Press: Oxford, 2005.
14. Franca LP, Frey S. Stabilized finite element methods: II. The incompressible Navier–Stokes equations. *Computer Methods in Applied Mechanics and Engineering* 1991; **99**:209–233.
15. Hughes TJR, Brooks A. Streamline upwind/Petrov–Galerkin formulation for convection dominated flows with particular emphasis on the incompressible Navier–Stokes equations. *Computer Methods in Applied Mechanics and Engineering* 1982; **32**:199–259.
16. Hughes TJR, Brooks A. A theoretical framework for Petrov–Galerkin methods with discontinuous weighting functions: application to the streamline-upwind procedure. In *Finite Elements in Fluids*, Gallagher RH *et al.* (eds). vol. 4. Wiley, 1982; 47–65.
17. Jansen K, Collis SS, Whiting C, Shakib F. A better consistency for low-order stabilized finite element methods. *Computer Methods in Applied Mechanics and Engineering* 1999; **174**:153–170.
18. Bochev P, Gunzburger M, Lehoucq R. On stabilized finite element methods for transient problems with varying time scales. *Proceedings of ECOMASS 2004*; *European Congress on Computational Methods in Applied Sciences and Engineering*, 2004.
19. Bochev P, Gunzburger M, Shadid J. On inf–sup stabilized finite element methods for transient problems. *Computer Methods in Applied Mechanics and Engineering* 2004; **193**:1471–1489.
20. Franca LP, Valentin F. On an improved unusual stabilized finite element method for the advective–reactive–diffusive equation. *Computer Methods in Applied Mechanics and Engineering* 2000; **190**:1785–1800.
21. Franca LP, Dutra Do Carmo EG. The Galerkin gradient least-squares method. *Computer Methods in Applied Mechanics and Engineering* 1989; **74**:41–54.
22. Franca LP, Ramalho JVA, Valentin F. Multiscale and residual-free bubble functions for reaction-advection-diffusion problems. *International Journal for Multiscale Computational Engineering* 2005; 3(3):297–312.
23. Hauke G, Doweidar MH. Fourier analysis of semi-discrete and space-time stabilized methods for the advective–diffusive–reactive equation: III. SGS/GSGS. *Computer Methods in Applied Mechanics and Engineering*, in press.
24. Harari I. Stability of semidiscrete formulations for parabolic problems at small time steps. *Computer Methods in Applied Mechanics and Engineering* 2004; **193**(15–16):1491–1516.
25. Codina R, Vázquez M, Zienkiewicz OC. A general algorithm for compressible and incompressible flows. Part III: the semi-implicit form. *International Journal for Numerical Methods in Fluids* 1998; **27**:13–32.
26. Ciarlet P. The finite element method for elliptic problems. *SIAM Classics in Applied Mathematics* SIAM: Philadelphia, 2002.
27. Brezzi F. On existence, uniqueness and approximation of saddle-point problems arising from Lagrange multipliers. *Mathematical Modeling and Numerical Analysis* 1974; **21**:129–151.
28. Bochev P, Lehoucq R. Regularization and stabilization of discrete saddle-point variational problems. *Electronic Transactions on Numerical Analysis* 2006; **22**:97–113.
29. Brezzi F. Stability of saddle-points in finite dimensions. In *Frontiers in Numerical Analysis*, Blowey J, Craig A, Shardlow T (eds). Springer: Berlin, 2002; 17–61.
30. Brezzi F, Bathe K-J. A discourse on the stability conditions for mixed finite element formulations. *Computer Methods in Applied Mechanics and Engineering* 1990; **82**:27–57.

DOI: 10.1002/fld

31. Shakib F, Hughes TJR. A new finite element formulation for computational fluid dynamics: IX. Fourier analysis of space-time Galerkin/least-squares algorithms. *Computer Methods in Applied Mechanics and Engineering* 1991; **87**:35–58.
32. Shakib F, Hughes TJR, Johan Z. A new finite element formulation for computational fluid dynamics: X. The compressible Euler and Navier–Stokes equations. *Computer Methods in Applied Mechanics and Engineering* 1991; **89**:141–219.
33. Bochev P, Lehoucq R. On the finite element solution of the pure Neumann problem. *SIAM Review* 2005; **47**:50–66.
34. Brezzi F, Pitkaranta J. On the stabilization of finite element approximations of the Stokes problem. In *Efficient Solutions of Elliptic Systems*, Hackbusch W (ed.). Notes on Numerical Fluid Mechanics, vol. 10. Braunschweig: Wiesbaden, Viewig, 1984; 11–19.
35. Golub G, Van Loan C. *Matrix Computations* (3rd edn). Johns Hopkins University Press: Baltimore, MD, 1996.
36. Brezzi F, Fortin M. *Mixed and Hybrid Finite Element Methods*. Springer: Berlin, 1991.
37. Hughes TJR, Feijoo GR, Mazzei L, Quincy JB. The variational multiscale method: a paradigm for computational mechanics. *Computer Methods in Applied Mechanics and Engineering* 1998; **166**:3–24.
38. Dohrmann C, Bochev P. A stabilized finite element method for the Stokes problem based on polynomial pressure projections. *International Journal for Numerical Methods in Fluids* 2004; **46**:183–201.
39. Bochev P, Dohrmann C, Gunzburger MD. Stabilization of low-order mixed finite elements for the Stokes equations. *SIAM Journal on Numerical Analysis* 2006; **44**(1):82–101.
40. Silvester DJ, Kechkar N. Stabilized bilinear-constant velocity–pressure finite elements for the conjugate gradient solution of the Stokes problem. *Computer Methods in Applied Mechanics and Engineering* 1990; **79**:71–86.
41. Silvester DJ. Optimal low order finite element methods for incompressible flow. *Computer Methods in Applied Mechanics and Engineering* 1994; **111**:357–368.
42. Hughes TJR, Stewart J. A space-time formulation for multiscale phenomena. *Journal of Computational and Applied Mathematics* 1996; **74**:217–229.
43. Stoyan G. Towards discrete Velte decompositions and narrow bounds for inf–sup constants. *Computers and Mathematics with Applications* 1999; **38**:243–261.

DOI: 10.1002/fld